Engineering Reports

WILEY

Engineering Reports
Open Access

RESEARCH ARTICLE OPEN ACCESS

Innovative Diversity Metrics in Hierarchical Population-Based Differential Evolution for PEM Fuel Cell Parameter Optimization

Mohammad Khishe[1,2,3] | Pradeep Jangir[4,5,6] | Arpita[7] | Sunilkumar P. Agrawal[8] | Sundaram B. Pandya[9] | Anil Parmar[9] | Laith Abualigah[10]

[1]Department of Electrical Engineering, Imam Khomeini Naval Science University of Nowshahr, Nowshahr, Iran | [2]Innovation Center for Artificial Intelligence Applications, Yuan Ze University, Taoyuan City, Taiwan | [3]Jadara University Research Center, Jadara University, Irbid, Jordan | [4]University Centre for Research and Development, Chandigarh University, Mohali, India | [5]Department of CSE, Graphic Era Deemed to be University. Graphic Era Hill University, Dehradun, Uttarakhand, India | [6]Applied Science Research Center, Applied Science Private University, Amman, Jordan | [7]Department of Biosciences, Saveetha School of Engineering, Saveetha Institute of Medical and Technical Sciences, Chennai, India | [8]Department of Electrical Engineering, Government Engineering College, Gandhinagar, Gujarat, India | [9]Department of Electrical Engineering, Shri K.J. Polytechnic, Bharuch, India | [10]Computer Science Department, Al al-Bayt University, Mafraq, Jordan

Correspondence: Mohammad Khishe (m_khishe@alumni.iust.ac.ir)

Received: 22 August 2024 | **Revised:** 11 November 2024 | **Accepted:** 14 November 2024

Funding: The authors received no specific funding for this work.

Keywords: differential evolution | HPDE | parameter estimation | PEMFC | proton exchange membrane fuel cell

ABSTRACT

The optimization of parameters in proton exchange membrane fuel cell (PEMFC) models is essential for enhancing the design and control of fuel cells and is currently a vibrant area of research. This involves a complex, nonlinear, and multivariable numerical optimization challenge. Recently, various metaheuristic approaches have been applied to efficiently identify optimal configurations for PEMFC models, capable of exploring a broad search space to locate ideal solutions promptly. In this study, the recently developed hierarchical population-based differential evolution (HPDE) was employed for parameter optimization of PEMFCs due to its robustness and demonstrated superiority over other optimization algorithms. This research tested the proposed optimization algorithm by identifying parameters for 12 distinct PEMFCs, including BCS 500 W PEMFC, Nedstack 600 W PS6 PEMFC, SR-12500 W PEMFC, H-12 PEMFC, STD 250 W PEMFC, and HORIZON 500 W PEMFC, four variants of 250 W PEMFC, and two variants of H-12 12 W PEMFC. The performance of HPDE was also benchmarked against other advanced evolutionary algorithms (EAs), such as E-QUATRE, iLSHADE, CRADE, L-SHADE, jSO, HARD-DE, LSHADE-cnEpSin, DE, and PCM-DE. Despite its simplicity, the results reveal that HPDE can precisely and swiftly extract the parameters of PEMFC models. Furthermore, the voltage–current (V–I), power-current (P–I), and error characteristics derived from the HPDE algorithm consistently align with both simulated and experimental data across all seven models of PEMFCs. Additionally, HPDE has shown to outperform various versions of DE algorithms, providing superior results.

1 | Introduction

For the past years, the desire for more energy throughout the world, fall down of traditional sources of fuel and care about the environment has been so good that it has led to great emphasis on fuel cell technology [1, 2]. Fuel cells are highly acclaimed because they can help cure energy shortage; these cells generate electricity by means of electrochemical reactions, as opposed to conventional combustion processes [3]. Modeling proton exchange membrane fuel cells (PEMFCs) have become popular as it allows better prediction of cell performance and understanding of different phenomena than experimental approaches [4]. On the other hand, it is not easy to predict PEMFC characteristics correctly due to their strong dependence on operational conditions [5]. Traditional modeling methods often fail to cope with complex, nonlinear, and multivariable PEMFCs and their interdependencies [6]. Hence, metaheuristic (MH) optimization algorithms, which have shown adaptability and robustness, are becoming increasingly common in PEMFC modeling [7].

Much research has been done on parameter optimization modeling for PEMFCs by using normal methods and also sophisticated MH algorithms. The classification of $V-I$ characteristics from these models into steady state and dynamic states is made. Both these states are well captured in a comprehensive mathematical model recommended in [8]. For example, referring to Nernst voltage or thermodynamic potentials as static elements alongside concentration and activation voltages as transient components renders the steady state $V-I$ characteristics through an electrochemical model. Second-order least square polynomials represent static components, while the transient elements use fifth-order polynomials with coefficients obtained from the least square method. Consequently, steady state $V-I$ characteristics are determined by combining both static and transient components, whereas dynamic characteristics are indicated by first-order time delay.

Moreover, this is a PEMFC system that is semi-empirical single input and single output and provides for real-time parameter identification as described in [9], while PEOFC parameters estimation by means of particle swarm optimization (PSO) algorithm can be found in [10]. In the parameter identification phase, the Levenberg–Marquardt algorithm and Gauss–Newton method are other traditional methods used to solve nonlinear equations. For both noisy and noise-free cases, 20,000 iterations were done on different operational settings to obtain solutions.

Using MATLAB, a Nexa 1.2 kW model that consists of 47 cells has been simulated allowing for the evaluation of five different PEMFC parameters as indicated in [11]. Additionally, this calls for brief review discussion on parameter estimation using genetic algorithm (GA) variations and other methods in this field found in [12]. For example, thermal conductivity and relative humidity are determined after performing simulations under four pressure levels that are significantly distant from each other and satisfactory results are received by 250 iterations.

PEMFCs have been observed to possess higher power outputs upon the inclusion of nano coolants, as seen from the $V-I$ characteristics given [13]. However, this study compares the performance of GAs in estimating parameters to conventional curve fitting techniques explained in [14]. To ensure an extensive analysis, various $V-I$ characteristic curves were plotted at different operating points to verify parameter identification and verification.

In [15], the maximum power point method is recommended for parameter identification, while Transferred Adaptive Differential Evolution (TRADE) is employed for parameter estimation of both SOFCs and PEMFCs [16]. Bee swarm algorithm (BSA), used in extracting PEMFC parameters [17], registers negligible error margins against PSO, revealing its improved efficiency due to variation in scaling factor.

For PEMFC parameter estimation, Grey Wolf Optimization (GWO) outperforms other algorithms, as shown in [18]. On top of using GWO to optimize performance further, a chaotic enhancement technique has been incorporated into it with a view of enhancing the convergence rate while maintaining diversity within the SOFC population, as studied by [19]. Moth flame optimization algorithm (MFOA) was used for extracting PEMFC parameters, which favorably competed with PSO and sine cosine algorithm (SCA), respectively, using four statistical metrics but achieved the lowest standard deviation for SR-12 and Nedstack PS-6 PEMFC models [20].

Salp swarm algorithm (SSA) is implemented for parameter identification [21], validating the optimization method's efficacy across varied operating pressures and temperatures for two commercial PEMFC models, aligning closely with experimental curves. The bald eagle search (BES) algorithm, mimicking the predatory strategies of bald eagles, is used in [22] for PEMFC parameter estimation. This three-phase method (Selection, Search, and Swooping) has demonstrated a reduced error rate and improved convergence across diverse operational scenarios. BES achieved an exceptionally low fitness value of 0.01136 in extracting parameters for the BCS 500 W and Nedstack PS6 models, as noted in [23].

An advanced version of the Barnacles Mating Optimizer (BMO) incorporating Levy Flight mechanics and chaos theory is proposed in [24] for enhanced parameter identification. This innovative approach, drawing inspiration from barnacles' mating behaviors, utilizes the Hardy Weinberg equilibrium for progeny generation, showing significant error reduction when compared against other prominent algorithms such as Elephant Herding Optimization, Emperor Penguin Optimizer, and World Cup Optimization, particularly for the Nedstack PS6 and Horizon 500 W FC systems.

Parameter estimation in PEMFCs is further refined using the Slime Mould Algorithm (SMA) [25], and parameters are extracted employing the Marine Predator Algorithm (MPA) and Political Optimizer (PO) algorithm, which operate in three and five phases, respectively, as detailed in [26]. The polarization curves for PEMFC are documented under varying conditions. Additionally, the Mayfly Optimization Algorithm (MOA), enhanced with chaotic mapping, is tailored for optimal parameter design in PEMFC, as presented in [27]. This innovative hybrid algorithm ensures optimal operational parameters, enhancing overall efficiency and performance.

Chaotic mapping reduces the initial population size, enhancing the optimization process with the disorder mayfly method. The

MOA represents an adaptation of PSO. The literature showcases a plethora of bio-inspired algorithms employed for parameter estimation in PEMFC models. These include the Tree Growth Algorithm [28], Whale Optimization Algorithm [29], Chaos Owl Search Algorithm (COSA) [30], Artificial Bee Swarm Optimization (ABSO) [31], Modified Farmland Fertility Optimization Algorithm (MFFA) [32], Developed Sunflower Optimization Algorithm [33], Improved Harris Hawks Optimization Algorithm (IHHO) [34], Hunger Games Search Algorithm [35], Pathfinder algorithm (PFA) [36], Black Widow Optimization (BWO) [37], Ant lion Optimizer (ALO) and Dragon Fly Algorithm (DA) [38], and Improved Chicken Swarm Optimization Algorithm [39].

System identification for the PEMFC stack has been effectively carried out in [40] using a hybrid configuration of PSO and Emperor Penguin Operator to ascertain optimal parameters that reflect true output voltage values. Despite the extensive development of MH algorithms, details on their specific applications, suitability, and efficiency often remain fragmented. The utility of MHs in extracting parameters for PEMFC models showcases the diverse array of optimization methods developed by researchers. There is an ongoing imperative to innovate or refine existing algorithms to meet diverse challenges. Present efforts are aimed at devising a unique, more accurate, and reliable metaheuristic algorithm (MA) capable of addressing various optimization challenges comprehensively, highlighting the challenge that while one technique may excel in certain scenarios, it might underperform in others. In the past few years, many optimization techniques have been applied to improve the efficiency and effectiveness of energy systems, such as Combined Cooling, Heating, and Power (CCHP) systems and microgrid scheduling. An improved mother optimization algorithm to evaluate the efficiency of CCHP systems in the Xinjiang Uygur Autonomous Region is proposed by Li et al. [41]. In this approach, energy distribution within integrated energy systems was refined, resulting in significant operational improvements. In the same way, economic scheduling for microgrids is important, particularly in renewable energy environments. This issue was addressed by Jiang et al. [42], who developed an energy hub model coupled with demand response and an improved water wave optimization algorithm to solve the problem. As renewable energy integration into microgrids becomes more intense, this model presents a robust framework for efficient scheduling. In watersport complexes, Chen et al. [43] investigated optimization inside combined cooling, heating, and power systems using the African Vulture Optimization Algorithm. They showed that energy management strategies are effective, but that specialized optimization approaches are necessary for specific use cases, such as recreational or commercial facilities. The advancements in fuel cell modeling include progress in fuel cell modeling through machine learning techniques. Proton-exchange membrane fuel cells were modeled by combining a convolutional neural network with an extreme learning machine, optimized by an improved Honey Badger algorithm [44]. The hybrid approach allowed for precise identification and performance prediction in fuel cells, with the value of AI-based optimizations demonstrated. Innovative configurations for maximum efficiency are needed for renewable energy systems, especially those that include wind, solar, and fuel cell power sources. An amended Dragon Fly optimization algorithm for structuring such hybrid systems was developed by Bo et al. [45] for combined wind, photovoltaic, and fuel cell systems. The results showed that optimized structures could greatly improve energy outputs under different environmental conditions. Decarbonization requires the evolution of energy grids to smart grids or an Internet of Energy. Ghiasi et al. [46] provide a conceptual model for this transformation, which includes enhanced interconnectivity and digitalized energy management, and clearly defines the path toward deep decarbonization in the energy sector. In addition, recent research advances which are related to the application of HPDE algorithm in PEMFC optimization will be included in the literature review to strengthen it. For example, health management of PEMFC systems during long-term operation studies shows the importance of optimal temperature trajectory optimization to maintain performance, supporting the need for robust parameter optimization methods such as HPDE to maintain stability over long periods of time [47]. Further, recent advances in online diagnostic methods [48], including water management fault detection using hybrid-frequency electrochemical impedance spectroscopy, highlight the need for advanced optimization algorithms for real-time PEMFC management. Including these references will also help in giving a broader context of the latest challenge and the key advantage that HPDE offers to PEMFC parameter identification for use in the field.

In the present paper, one of the MAs that is most useful for parameter identification in PEMFCs is hierarchical population-based differential evolution (HPDE) with a novel diversity metric [49]. The algorithm has been validated extensively on 88 benchmark functions from CEC2013, CEC2014, and CEC2017 suites, where it either matched or outperformed six leading DE variants. In this paper, we examine performance of HPDE algorithm in extracting PEMFC parameters against established DE variants like E-QUATRE [50], iLSHADE [51], CRADE [52], L-SHADE [53], jSO [53], HARD-DE [54], LSHADE-cnEpSin [55], DE [56] and PCM-DE [57].

The complex, nonlinear, and multivariable nature of PEMFC models makes the application of the majority of parameter estimation methods, such as the Levenberg–Marquardt algorithm and the Gauss–Newton method, difficult. Due to the strong dependence of PEMFC performance on operating conditions and the inherent limitations of these conventional techniques in handling nonlinear dynamics, these conventional techniques are less effective for accurately capturing PEMFC performance. The PEMFC parameter estimation is a complex, multivariable problem, and therefore MAs have proven to be robust tools for handling such problems. Traditional methods cannot cover a wide search space, and they provide the adaptability needed to explore diverse operating conditions. As such, MH approaches are being increasingly used to optimize PEMFC models, and this research is motivated to extend the capability of this by developing a novel, more effective algorithm. Estimation of PEMFC parameters is critical to improving the performance, efficiency, and reliability of fuel cells in practical applications. As a sustainable energy solution, PEMFCs are poised to be used in the real world; optimal parameter estimation plays an important role in determining power output, durability, and control accuracy, and is a key factor in advancing PEMFC technology for real-world use. Due to the high expectations of efficiency and convergence in PEMFC modeling, current methods tend to suffer from convergence speed, error minimization, and consistency across different PEMFC models. Such a high-performance optimization algorithm that consistently achieves these goals can propel fuel cell technology and deployment. In this study, HPDE is introduced as a newly developed algorithm that specifically addresses the need to improve the convergence, accuracy, and stability of the parameter estimation. A structured population hierarchy and novel mutation strategies are used by HPDE to achieve a balanced exploration and exploitation. The hierarchical design is intended to improve convergence rates while remaining robust to premature convergence, a common problem in other MAs. To demonstrate the effectiveness and superiority of HPDE, the study rigorously benchmarks HPDE against several other well-regarded evolutionary algorithms (EAs), including E-QUATRE, iLSHADE, and others. This work aims to show that HPDE not only achieves but outperforms these benchmark algorithms in terms of accuracy, convergence speed, and stability across a variety of PEMFC models. The real-world applicability of HPDE is validated against experimental and simulated data of 12 different PEMFC types. Comparisons of voltage current ($V-I$) and power current ($P-I$) characteristics are made, and they match well with experimental results, demonstrating that HPDE is effective in practically real-time PEMFC parameter estimation. PEMFCs are a promising technology as the world looks for sustainable energy sources. Maximizing PEMFC efficiency requires accurate and efficient parameter estimation, and HPDE's contributions are directly relevant to the broader energy landscape. The objective of this study is to improve PEMFC performance and to support the transition to cleaner, more sustainable energy solutions.

The notable feature of HPDE is its robustness and superior performance in optimizing PEMFC parameters. In this study, various PEMFC models have been considered, including BCS 500 W PEMFC [58], Nedstack PS6 [59], S-12500 W PEMFC [60], H-12 PEMFC [61], STD 250 W PEMFC [62], and HORIZON 500 W PEMFC [63]. This research makes several important contributions:

1. Introduction of HPDE for PEMFC Parameter Optimization: HPDE is an innovative approach to the DE algorithms for the challenging PEMFC parameter estimation task. To the best of our knowledge, this is the first application of HPDE in this domain, differentiating it from previously known DE variants, as well as other EAs. The hierarchical population mechanism and novel mutation strategies are designed to well balance the exploration and exploitation, which can improve the convergence rate and accuracy. These capabilities are critical for PEMFC modeling, where parameter estimation precision directly translates into performance and operational efficiency.
2. Novel Hierarchical Population Structure: HPDE is a dynamic two-layer hierarchical population structure that divides the population into elite and ordinary layers according to individual performance. The hierarchical arrangement of HPDE enables the concentration of resources on promising solutions (elite layer) while preserving diversity in the entire population (ordinary layer), which is a common problem of DE algorithms: premature convergence. The structural innovation encourages robust convergence, which is critical in the highly nonlinear, multivariable environment of PEMFC models.
3. Innovative Diversity Metric and Control Mechanisms: Another contribution presents a novel diversity metric introduced in HPDE to optimize the population diversity dynamically during the evolution. This metric allows us to tune the algorithm to adapt to the measurements of the diversity of the search space and spread of the population. In PEMFC parameter estimation, such adaptability is essential because of the variations in operating conditions, requiring a flexible optimization approach that is able to cope with a large spectrum of system dynamics.
4. Enhanced Mutation and Selection Strategies: HPDE's mutation strategy, which distinguishes between elite-guided and ordinary-guided mutation, enables a finer exploration of the solution space, improving both convergence speed and solution quality. Moreover, the selection strategy involves suboptimal solutions to enhance the ability of the algorithm to get out of local optima, a crucial enhancement compared to conventional DE strategies. These improvements guarantee that HPDE can generate solutions with little error and therefore more trustworthy parameter estimates than other methods.
5. Comparative Analysis with Leading DE Variants and EAs: HPDE is compared to nine well-known EAs, including the best DE variants, such as E-QUATRE, iLSHADE, and CRADE. This thorough comparison shows HPDE's effectiveness and its superiority in terms of minimum error, runtime, and stability. HPDE always performs better, making it a competitive advantage and proving its novelty as a better optimization tool for PEMFCs.
6. Practical Validation Across Multiple PEMFC Models: In this study, HPDE is used for parameter estimation in 12 different PEMFC types from commercial to laboratory models, and consistent alignment between estimated and experimental $V-I$ and $P-I$ characteristics is obtained. Extensive validation confirms the practical applicability and effectiveness of HPDE over a wide range of PEMFC configurations, which is a significant step forward in view of the wide range of operating conditions and performance requirements in PEMFC systems.

The paper is structured to provide a succinct overview of the PEMFC stack model and the optimization goals in Section 2, an introduction to the HPDE algorithm in Section 3, detailed experimental analyses and discussions in Section 4, and conclusions in Section 5.

2 | Problem Formulation

In this section, we provide an overview of the PEMFC stack model utilized in this study, followed by the specification of the objective function to be optimized.

2.1 | PEMFC Stack Model

PEMFC stack model described in [62] is based on an electrochemical framework for predicting steady-state performance and is specifically developed to be computationally manageable and suitable for engineering optimization tasks. This model consists of basic PEMFC components such as the electrochemical reaction sites (cathode and anode), membrane, and related voltage losses. The model makes essential assumptions of ideal gas behavior of reactants, uniform temperature, and pressure distribution across the stack, and simplifications for water management and thermal effects. The formulation of the model includes calculating the stack output voltage as a function of current, anode and cathode pressures, and reaction kinetics, with overpotential losses (activation, ohmic, and concentration) included. The model can be adjusted by parameters to match empirical data and is flexible in engineering applications and practical in optimizing performance under different operating conditions. The PEMFC stack model referenced in [62] is employed in this study. For a stack comprising n cells connected in series, the terminal voltage can be determined using [63]:

$$V_s = n \cdot V_{FC}, \tag{1}$$

where V_{FC} is the output voltage of a single cell, which can be formulated as [64].

$$V_{FC} = E_{Nernst} - V_{act} - V_{ohm} - V_{con}, \tag{2}$$

E_{Nernst} is the thermodynamic potential defined by

$$E_{Nernst} = 1.229 - 0.85 \times 10^{-3} \cdot (T - 298.15) + 4.3085 \times 10^{-5} \cdot T \cdot \ln\left(P^*_{H_2} \sqrt{P^*_{O_2}}\right), \tag{3}$$

where T is the cell temperature (K), $P^*_{H_2}$ and $P^*_{O_2}$ are the hydrogen and oxygen partial pressures (atm), respectively. They are given by [65].

$$P^*_{H_2} = 0.5 \cdot RH_a \cdot P^{sat}_{H_2O} \cdot \left(\frac{1}{\frac{RH_a \cdot P^{sat}_{H_2O}}{P_a} \exp\left(\frac{1.635(i_{cell}/A)}{T^{1.334}}\right)} - 1 \right), \tag{4}$$

$$P^*_{O_2} = RH_c \cdot P^{sat}_{H_2O} \cdot \left(\frac{1}{\frac{RH_c \cdot P^{sat}_{H_2O}}{P_c} \exp\left(\frac{4.192(i_{cell}/A)}{T^{1.334}}\right)} - 1 \right), \tag{5}$$

where RHa and RHc are the relative humidity of vapor in the anode and cathode, Pa and Pc are the anode and cathode inlet pressures (atm), respectively. A is the effective electrode area (cm^2) and i_{cell} is the cell current (A). $P^{sat}_{H_2O}$ is the saturation pressure of water vapor (atm), which is defined as a function of the temperature T as follows [62, 66].

$$\log_{10}\left(P^{sat}_{H_2O}\right) = 2.95 \times 10^{-2} \cdot (T - 273.15) - 9.19 \times 10^{-5} \cdot (T - 273.15)^2 + 1.44 \times 10^{-7} \cdot (T - 273.15)^3 - 2.18. \tag{6}$$

According to reference [67], the activation overpotential V_{act}, including anode and cathode, can be expressed by the following formula

$$V_{act} = -\left[\xi_1 + \xi_2 \cdot T + \xi_3 \cdot T \cdot \ln\left(C^*_{O_2}\right) + \xi_4 \cdot T \cdot \ln\left(i_{cell}\right)\right], \tag{7}$$

where $\xi 1, \xi 2, \xi 3, \xi 4$ are the parametric coefficients for each cell model, and $C^*_{O_2}$ (mol/cm^3) is the concentration of oxygen in the catalytic interface of the cathode, given by [62, 64].

$$C^*_{O_2} = \frac{P^*_{O_2}}{5.08 \times 10^6 \cdot \exp(-498/T)}. \tag{8}$$

The ohmic voltage drop V_{ohm} can be determined by the following expression [67].

$$V_{ohm} = i_{cell} \cdot \left(R_M + R_C\right), \tag{9}$$

where R_M is the equivalent membrane resistance to proton conduction, and R_C is the equivalent contact resistance to electron conduction. R_M is defined by [62].

$$R_M = \frac{\rho_M \cdot \ell}{A}, \tag{10}$$

$$\rho_M = \frac{181.6 \cdot \left[1 + 0.03 \cdot \left(\frac{i_{cell}}{A}\right) + 0.062 \cdot \left(\frac{T}{303}\right) \cdot \left(\frac{i_{cell}}{A}\right)^{2.5}\right]}{\left[\lambda - 0.634 - 3 \cdot \left(\frac{i_{cell}}{A}\right)\right] \cdot \exp\left[4.18 \cdot \left(\frac{T-303}{T}\right)\right]}, \tag{11}$$

where ρ_M is the membrane-specific resistivity for the flow of hydrated protons (Ω cm), and ℓ is the thickness of the membrane (cm), which serves as the electrolyte of the cell. The parameter λ is an adjustable parameter with a possible range of references [66, 68].

The concentration overpotential V_{con} caused by the change in the concentration of the reactants at the surface of the electrodes as the fuel is calculated by [64].

$$V_{con} = -B \cdot \ln\left(1 - \frac{J}{J_{max}}\right), \tag{12}$$

where B (V) is a parametric coefficient, which depends on the cell and its operation state. J is the actual current density of the cell (A/cm^2), and J_{max} is the maximum value of J.

The aim of parameter identification is to extract the unknown parameters of the PEMFC stack model to achieve a better fit for a given stack model. Similar to the approaches in [68–70], this work identifies seven parameters, that is, $\xi 1, \xi 2, \xi 3, \xi 4, \lambda, RC$, and B, will be identified by the HPDE algorithm.

2.2 | Objective Function

In order to determine the optimal values for the seven unknown parameters mentioned above through optimization techniques, an objective function must be defined. In this study, the objective function is the SSE (sum of squared errors) between the actual output voltage of the PEMFC stack and the model output voltage, defined as [23]:

$$\min f(\mathbf{x}) = \sum_{k=1}^{N} \left(V_{sm,k} - V_{so,k}\right)^2, \tag{13}$$

where $x = \{\xi_1, \xi_2, \xi_3, \xi_4, \lambda, R_C, B\}$: This vector x represents the seven unknown parameters to be identified within the PEMFC model. These parameters affect various aspects of the model, such as activation overpotential, ohmic resistance, and concentration overpotential, which influence the fuel cell's voltage output. $V_{sm,k}$: The actual stack voltage from experimental data at the kth measurement point. This value serves as the reference voltage for the model, reflecting real PEMFC performance under specific conditions. $V_{so,k}$: The modeled output voltage at the kth measurement point. This is the voltage predicted by the PEMFC model based on current parameter values. N: The number of data points available from experimental measurements, used to calculate the error between actual and modeled voltages across various operating points. The objective function aims to find the optimal parameter values that minimize the total error between the experimental (actual) and modeled voltages across all data points. The error at each data point k is represented as $\left(V_{sm,k} - V_{so,k}\right)^2$, and summing these errors over all N data points provide the overall SSE. minimizing SSE, the overall discrepancy between the actual PEMFC performance and the modeled performance is reduced, thus improving the accuracy of the model in representing the fuel cell behavior.

3 | The Proposed HPDE Algorithm

This section provides an in-depth explanation of the newly developed dynamic HPDE algorithm, which introduces a novel diversity metric. The description is divided into four parts: the first part describes the dynamic hierarchical population mechanism; the second part introduces the diversity metric; the third part explores innovative mutation strategies; and the fourth part discusses enhancements in parameter control through dimension improvement.

3.1 | The Dynamic Hierarchical Population

In the HPDE algorithm, the population is divided into two layers: the elite layer $\mathrm{lay_e}$ and ordinary layer $\mathrm{lay_o}$, based on the performance of each individual within the population. Two parameters, EP and OP, represent the sizes of these two layers, respectively. Additionally, a parameter, IS (Individual Status), is introduced to categorize individuals into different layers. The value of IS is calculated using via Equation (14):

$$\mathrm{IS} = \frac{\left| f\left(\mathbf{x}^g_{\mathrm{aver}}\right) - f\left(\mathbf{x}^g_i\right) \right|}{f\left(\mathbf{x}^g_{\mathrm{worst}}\right) - f\left(\mathbf{x}^g_{\mathrm{best}}\right)}, \tag{14}$$

where $f\left(\mathbf{x}^g_i\right)$, $f\left(\mathbf{x}^g_{\mathrm{best}}\right)$, and $f\left(\mathbf{x}^g_{\mathrm{worst}}\right)$ denote fitness value of current individual, best individual, and worst individual, respectively. The IS value is constrained to the range [0, 1] throughout the entire evolution process. Individuals with an IS value exceeding a certain threshold are placed in the elite layer, while the remaining individuals are assigned to the ordinary layer. The lower and upper bounds calculated using Equations (15) and (16), respectively:

$$\mathrm{Low}_i = \left\lfloor w_1 \cdot ps \cdot \left(1 - \frac{nfe}{nfe_{max}}\right)\right\rfloor, \tag{15}$$

$$\mathrm{Up}_i = \left\lfloor w_2 \cdot ps \cdot \left(1 - \frac{nfe}{nfe_{max}}\right)\right\rfloor + \delta, \tag{16}$$

where Low_i and Up_i represent the upper bound and lower bound of the algorithm. The pseudo-code for generating the dynamic hierarchical population is provided in Algorithm 1.

ALGORITHM 1 | The pseudo-code of the population dynamic division mechanism.

Input: *P,ps,nfemax,nfe,oct, D*
Output: *The two layers lay, layo and their size EP, OP*
  Initial value $oct = 0$, $EP = 0$, $OP = 0$;
  for $i = 1$ *to ps* ***do***
    Calculation of IS as shown in ***Eq. (14)***;
    if $IS < 0.1$ ***then***
      $EP = EP + 1$;
    end if
  end for
  if $EP > Upi$ *or* $EP < Lowi$ ***then***
    $EP = \left\lfloor (Upi - Lowi) \cdot \frac{nfemax - nfe}{nfemax} + Lowi \right\rfloor$;
  end if
  Calculate the size of ordinary layer: $OP = ps - EP$
  Sort the current parent population P in ascending order according to the fitness values; Return EP, OP, and layers laelayo of individuals;
  Return EP, OP, and layers laye layo of individuals

3.2 | The Diversity Metric

This section introduces a novel diversity metric for the population within our HPDE algorithm, based on the computation of two hyper-volumes: one hyper-volume, V_{lim} corresponds to the bound constraints of the search space, while the other, V_{pop} relates to the spatial distribution of the population during evolution. The calculation formulas of V_{lim} and V_{pop} are given in Equations (17) and (18):

$$V_{\mathrm{lim}} = ln\left(1 + \prod_{d=1}^{D} \left|u_d - l_d\right|\right), \tag{17}$$

$$V_{\mathrm{pop}} = \sqrt{\prod_{d=1}^{D} y_d}, \tag{18}$$

where u_i and l_i are the upper and lower bound of the ith dimension, and y_i denotes the distance between the maximum and minimum values of the ith dimension in the population. After the calculation of V_{lim} and V_{pop}, the diversity metric d_{vol} can be calculated via Equation (19):

$$d_{\mathrm{VOL}} = \sqrt{\frac{V_{\mathrm{pop}}}{V_{\mathrm{lim}}}}. \tag{19}$$

This simple equation shows that the diversity metric essentially calculates the ratio of the current population's diversity to that of the initial population. For further clarity, the proposed metric is described in detail in Algorithm 2.

ALGORITHM 2 | Calculation of the dVOL.

Data: *Individuals X1, G, …, Xi, G, …, Xps, G in the population*;
$Vpop = 1$
for $j = 1$ *to* D **do**
$q1 = \min(X(:,j))$
$q2 = \max(X(:,j))$;
$Vpop = Vpop \cdot (q2 - q1)$
end for
$Vpop = \ln(1 - Vpop)$
$dVOL = \sqrt{\frac{Vpop}{Vlim}}$
return *Diversity metric dVOL*

Furthermore, the individual is updated according to a greedy strategy shown in Equation (20):

$$U_{i,G} = X_{i,G} + F_{con} \cdot \left(X_{r_1,G}^{better} - X_{i,G}\right). \tag{20}$$

The performance improvement is bigger than N, $ct > N$, diversity improvement of the population should be launched according to Equation (21):

$$\begin{cases} X_{i,G+1} = X_{i,G} + F_{div} \cdot \left(X_{s_1,G} - X_{s_2,G}\right) & \text{if seed} \neq / \\ X_{i,G+1} = X^l + rand \cdot \left(X^u - X^l\right) & \text{otherwise} \end{cases}. \tag{21}$$

The diversity improvement factor, F_{div} follows a fixed Cauchy distribution $F_{\text{div}} \sim C(0.5,0.1)$, $X_{s_1,G}$ and $X_{s_2,G}$ are two unique seed individuals selected at random, while XX^u and X^l represent the upper and lower bounds of the population. The pseudo-code for the diversity metric-based population enhancement is provided in Algorithm 3.

ALGORITHM 3 | Pseudo-code of the diversity metric based population enhancement.

Input: $D, X^l, X^u, N, \xi, ct, f, ps, nfe, nfe_{max}$
Output: $nfe, nfe_{max}, ct, ps, f$
while $nfe < nfe_{max}$ **do**
if $round(d_{vol} * 10) == 5$ **then**
$num = round(0.15 * ps)$;
$nums = ceil(ps * rand(\ num))$:
$numst = pbest\ (\ nums, \ )$;
$seedstore = [\ seedstore\ ; numst]$;
end if
$seed = size(seedstore)$;
Calculate d_{vol} *using Eq.* (19);
if $d_{VOL} > \xi$ **then**
for $i = 1: ps$ **do**
if $ct(i) > N$ *and* $X_{i,G} \neq X_{gbest}$ **then**
$U_{i,G} = X_{i,G} + F_{\text{con}} \cdot \left(X_{r_1,G}^{\text{better}} - X_{i,G}\right)$;
Evaluate fitness value $f(U_{i,G})$
$nfe = nfe + 1$;
if $f(U_{i,G}) < f(X_{i,G})$ **then**
$X_{i,G+1} = U_{i,G}$, $ct(i) = 0$;
end if
end if
end for
else
for $i = 1: ps$ **do**
if $ct(i) > N$ *and* $X_{i,G} \neq X_{gbest}$ **then**
if $seed \neq \emptyset$ **then**
$X_{i,G+1} = X_{i,G} + F_{div} \cdot (X_{s_1,G} - X_{s_2,G})$;
else
$X_{i,G+1} = X^l + rand \cdot (X^u - X^l)$
end if
Calculate fitness value $f(X_{i,G+1})$, $ct(i) = 0$;
$nfe = nfe + 1$;
end if
end for
end if
end if
return $nfe, nfe_{max}, ct, ps, f$

3.3 | The Novel Mutation Strategies

The mutation strategy is a crucial factor in the effectiveness of the DE algorithm. The development of a robust DE variant often begins with the design of its mutation strategy. Typically, a successful DE variant strikes a balance between exploration and exploitation exploring the solution space in the early stages of evolution and focusing on local areas in the later stages. In the HPDE algorithm, elite individuals employ a novel mutation strategy designed to explore the objective landscape, while ordinary individuals utilize an enhanced "DE/target-to-best/1/bin" strategy to effectively explore the solution space. The rationale behind these strategies is that elite-guided mutation accelerates convergence and enhances exploitation, whereas ordinary-guided mutation increases population diversity and facilitates exploration. This approach ensures a balanced consideration of both exploration and exploitation in mutation strategies. The specifics of these two mutation strategies are detailed in Equation (22):

$$\begin{cases} V_{i,G} = X_{r_e,G} + p_w \cdot \left(X_{best,G}^{r_o} - X_{r_e,G}\right) + F \cdot \left(X_{r_e,G} - \hat{X}_{r_2,G}\right) \\ V_{i,G} = X_{r_o,G} + F \cdot \left(X_{best,G}^{p} - X_{r_o,G}\right) + F \cdot \left(X_{r_1,G} - \hat{X}_{r_2,G}\right) \end{cases}. \tag{22}$$

$X_{r_e,G}$ refers to a randomly selected individual from the elite layer, while $X_{best,G}^{r_o}$ is a randomly chosen individual from the top *EP*, also known as secondary elites, of the ordinary layer. The selection probability p_w is determined by the formula $p_w = \left(ps_{ini} - ps\right)/ps_{ini}$, $X_{r_o,G}$ represents a randomly selected individual from the ordinary layer, and $X_{r_1,G}$ is a randomly selected individual from the current population. The term $X_{best,G}^{p}$ denotes a randomly selected individual from the top $100p\%$ of the population, and $\hat{X}_{r_2,G}$ refers to a randomly selected individual from the combined pool of the current population and an external archive that uses a time-stamp mechanism, similar to the PaDE algorithm.

3.4 | Dimension Improvement-Based Parameter Control

In our algorithm, the process for generating control parameters F and CR varies according to the different layers of the population. For individuals in the ordinary layer, we establish a memory pool containing H entries that record recent μ_F and μ_{CR} pairs. The F and CR values are generated based on a semi-fixed Cauchy distribution $F \sim C(\mu_F, 0.1)$ and Gaussian distribution $\mathrm{CR} \sim N(\mu_{\mathrm{CR}}, 0.1)$ with the $\langle \mu_F, \mu_{\mathrm{CR}} \rangle$ pairs being randomly selected from the memory pool. Additional adjustments are needed to ensure that the scale factor F and the crossover rate CR stay within their respective ranges $F \in (0,1]$ and $CR \in [0,1]$. These adjustments are detailed in Equation (23).

$$F_i = \begin{cases} C(\mu_F, 0.1) & \text{while } F_i \leq 0 \\ 1 & if\ F_i > 1 \\ F_i & \text{otherwise} \end{cases} \tag{23}$$

$$\mathrm{CR}_i = \begin{cases} 0 & if\ \mu_{\mathrm{CR}} \leq 0 \parallel \mathrm{CR}_i < 0 \\ 1 & if\ \mu_{\mathrm{CR}} > 0 \&\& \mathrm{CR}_i > 1 \\ \mathrm{CR}_i & \text{otherwise} \end{cases} \tag{24}$$

For individuals in the elite layer, smaller CR and F values can enhance the algorithm's exploitation ability. Therefore, we propose a new approach using wavelet basis functions for generating F and a Gaussian-based method for generating CR, as outlined in Equations (25) and (26).

$$\mathrm{CR}_i = randn_i\left(2 \cdot \frac{ps}{ps_{ini}} \cdot \mathrm{IS}\right) \cdot \mathrm{CR}_i, \tag{25}$$

$$\begin{cases} F_i = \left(1 - \frac{0.5 \cdot nfe}{nfe_{max}}\right) \cdot \frac{2}{\sqrt{3}} \cdot \pi^{-\frac{1}{4}} \cdot (1 - \mu^2) \cdot e^{-\frac{\mu^2}{2}} \\ \mu = 2.5 \cdot \frac{nfe}{nfe_{max}} \cdot IS \end{cases}, \tag{26}$$

where ps denotes the current population, ps_{ini} denotes the initial population, IS denotes the individual status. the success rate is computed using Equation (27):

$$R_h = \begin{cases} \frac{n_{s,h}^2}{n_s \cdot (n_{s,h} + n_{f,h})} & if\ n_{s,h} > 0 \\ \varepsilon & \text{otherwise} \end{cases}, \tag{27}$$

where R_h represents the success rate of the hth entry, where n_s indicates the total number of successful individuals in the population. $n_{s,h}$ refers to the number of successful individuals utilizing the control parameter pair $\langle \mu_F, \mu_{\mathrm{CR}} \rangle$ from the hth entry, and $n_{f,h}$ denotes the number of individuals who failed while using the same control parameter pair. The adjustments to μ_F and μ_{CR} are then calculated using Equations (28) and (29).

$$\begin{cases} w_s = \frac{std(\Delta loc_i)}{\sum_{s=1}^{|S_F|} std(\Delta loc_i)} \\ \Delta loc_i = loc(U_{i,G} - X_{i,G}) \\ mean_{WL}(S_F) = \frac{\sum_{s=1}^{|S_F|} w_s \cdot S_F^2(s)}{\sum_{s=1}^{|S_F|} w_s \cdot S_F(s)} \\ \mu_{F,idx,G+1} = \begin{cases} mean_{WL}(S_F), & if\ S_F \neq \emptyset \\ \mu_{F,idx,G}, & otherwise \end{cases} \end{cases}. \tag{28}$$

$$\begin{cases} w_s = \frac{std(\Delta loc_i)}{\sum_{s=1}^{|S_F|} std(\Delta loc_i)} \\ \Delta loc_i = loc(U_{i,G} - X_{i,G}) \\ mean_{WL}(S_{CR}) = \frac{\sum_{s=1}^{|S_{CR}|} w_s \cdot S_{CR}^2(s)}{\sum_{s=1}^{|S_{CR}|} w_s \cdot S_{CR}(s)} \\ \mu_{CR,k,G+1} = \begin{cases} mean_{WL}(S_{CR}), & if\ S_{CR} \neq \emptyset \& max\{CR\} > 0 \\ 0, & if\ S_{CR} \neq \emptyset max\{CR\} = 0 \\ \mu_{CR,k,G}, & otherwise \end{cases} \end{cases}. \tag{29}$$

The symbols used in these equations carry the same meanings as previously described. The operator $loc(U_{i,G} - X_{i,G})$ measures the dimension improvements between the trial vector $U_{i,G}$ and the target vector $XX_{i,G}$. When it comes to population size ps, a rapid reduction at the start of the evolution often impairs effective exploration of the landscape. We further refined the PaDE reduction scheme, as outlined in Equation (30).

$$ps = \begin{cases} \left[\frac{ps_{\min} - ps_{ini}}{\left(\frac{2}{3} nfe_{\max} - ps_{ini}\right)^2} \cdot (nfe - ps_{ini})^2 + ps_{ini}\right], \\ if\ nfe \leq 0.5 \cdot nfe_{\max} \\ \left[\frac{ps_{\min} - \frac{1}{3} ps_{ini}}{\frac{1}{3} nfe_{\max}} \cdot (nfe - nfe_{\max}) + ps_{\min}\right], \\ \text{otherwise} \end{cases} \tag{30}$$

A step-by-step explanation of the HPDE algorithm:

1. Population Initialization: The initial population for the HPDE algorithm is generated by random sampling throughout the feasible search space of the PEMFC parameters. This population consists of each individual as a potential solution vector with parameters to be optimized. This initial population must be diverse enough to cover as broad area of the search space as possible preventing it from converging upon suboptimal solutions too early.

2. Dynamic Hierarchical Structure: The hierarchical structure of the HPDE algorithm is introduced by dividing the population into two main layers, the elite layer and the ordinary layer. In this, individuals are being divided based on the fitness values of the individuals of each generation. The individuals with higher fitness values (top performing) are assigned to the elite layer and the remaining individuals are assigned as ordinary individuals. Individuals are in dynamic motion between layers for the duration of the optimization process as their fitness values change from one generation to another.
   - Individual Status (IS) Calculation: The Individual Status (IS) is calculated for each individual as the relative difference between the individual's fitness value and the best and worst fitness values in the population. This IS value places an individual in either the elite or the ordinary layer of the hierarchical structure, and helps the structure to adapt.

3. Ranking-Based Mutation Operator: The mutation strategy used by the HPDE algorithm is unique and is designed to balance exploration and exploitation to deal with the complex landscape of PEMFC parameter optimization.
   - Elite-Guided Mutation: The elite layer individuals use a specialized mutation strategy to exploit high-quality

regions in the solution space. This mutation is an elite-guided mutation that focuses the algorithm on the areas with promising solutions and hence increases the convergence speed and accuracy of optimization.

- Ordinary-Guided Mutation: On the contrary, people in the ordinary layer use a mutation strategy that favors diversity, and thus encourages exploration of new areas in the solution space. This approach keeps the population diversity in the algorithm and prevents premature convergence, and helps the algorithm escape local optima.
- Greedy Selection Mechanism: The mutation strategy is complemented by a ranking-based selection mechanism that retains only the best solutions between the mutated and original individuals. The selection mechanism of this algorithm guarantees that the quality of each generation of the population is steadily improving, by refining the parameters of solutions of higher ranks.

4. Control Parameter Adaptation: In HPDE, control parameters like mutation factor (F) and crossover rate (CR) are dynamically adjusted using a novel method based on the distinction between elite and ordinary layers. Smaller F and CR values are used to fine-tune solutions for the elite layer, encouraging exploitation. On the other hand, larger F and CR values in the ordinary layer promote diversity for more exploration. Historical memory is then used to tune the control parameters further, incorporating successful past parameter values and improving adaptability and convergence stability.

5. Diversity Metric and Population Management: HPDE employs diversity metrics based on population spatial distribution in order to monitor and maintain diversity during the evolutionary process. The calculation of this metric via hyper volume comparisons allows the population to be effectively managed, allowing the algorithm to dynamically adjust the balance between exploration and exploitation.

4 | PEMFC Parameter Optimization—Experimental Analysis

In addition to the evolution matrix, the HPDE algorithm introduces a novel selection operator. This operator incorporates some suboptimal solutions during the evolution process, akin to selecting the top percentage of individuals in the population as part of the mutation strategy. This selection mechanism enhances the algorithm's ability to escape local optima during its evolutionary course. To validate the algorithm, a comprehensive test suite of 12 PEMFC fuel cell utilized, and the results underscore the enhanced performance of HPDE algorithm over the leading DE variants, including E-QUATRE [50], iLSHADE [51], CRADE [52], L-SHADE [53], jSO [53], HARD-DE [54], LSHADE-cnEpSin [55], DE [56], and PCM-DE [57], with default parameter settings are given in Table 1. All algorithms compared were set to their recommended to estimate the parameter of a PEMFC fuel cell BCS 500 W PEMFC [58], Nedstack PS6 [59], PEMFC, S-12500 W PEMFC [59], H-12 PEMFC [60], STD 250 W PEMFC [61], and HORIZON 500 W PEMFC [60] presented in Table 2. All the experiments are carried out on Matlab 2021a of a PC with Windows Server 2019 operating system CPU i7-11700k@3.6 GHz, maximum iterations 500, number of runs 30, and population size 40.

In order to evaluate the performance of HPDE compared to other benchmark algorithms, we analyze various metrics, including minimum, maximum, mean, standard deviation (std), runtime (RT), and Friedman Rank (FR), as presented in Table 3. HPDE achieves the best results with a minimum value of 0.0254927, the same as the best-performing algorithms like E-QUATRE, iLSHADE, CRADE, L-SHADE, jSO, and LSHADE-cnEpSin, and superior to PCM-DE and DE. The maximum value for HPDE is 0.0254927, indicating a consistent performance across different runs, outperforming other algorithms, which have higher maximum values like PCM-DE at 0.1757013 and E-QUATRE at 0.1924899. The mean value of HPDE is the lowest at 0.0254927, demonstrating its robustness and efficiency compared to others, with the next best mean being 0.0255143 from DE. The standard deviation of HPDE is 7.42E−09, showcasing an extremely stable performance, whereas other algorithms like HARD-DE and PCM-DE show higher variability with std. values of 0.0099976 and 0.045335, respectively. HPDE also excels in runtime, with an RT of 0.3451812 s, significantly faster than all other algorithms, with the closest being DE at 4.4975652 s. The Friedman Rank further confirms HPDE's superiority with a rank of 1, indicating the best overall performance among the algorithms evaluated. In comparison, algorithms like PCM-DE and E-QUATRE have much higher Friedman Ranks of 9.4 and 9.2, respectively. Overall, In Tables 3 and 4, HPDE not only shows exceptional performance across all metrics but also demonstrates remarkable stability and efficiency, clearly establishing it as the top-performing algorithm in this evaluation shown in Figure 1.

In order to evaluate the performance of FC1, HPDE compared to other benchmark algorithms, we analyze various metrics, including minimum, maximum, mean, standard deviation (std), runtime (RT), and Friedman Rank (FR), as presented in Table 5. HPDE achieves the best results with a minimum value of 0.275211, indicating superior performance compared to other algorithms like E-QUATRE, iLSHADE, CRADE, L-SHADE, jSO, HARD-DE, LSHADE-cnEpSin, DE, and PCM-DE. The maximum value for HPDE remains consistent at 0.275211, demonstrating

TABLE 1 | Recommended parameter settings of all these contrasted algorithms.

Algorithm	Parameters initial settings
LSHADE	$\mu F = 0.5$, $F \sim C\ (\mu F, 0.1)$, $\mu CR = 0.5$, $CR \sim C\ (\mu CR, 0.1)$, $ps = 18 \cdot D \sim 4$, $rrac = 2.6$, $p = 0.11$, $H = 6$
iLSHADE	$H, F, CR \& rrac$ same as LSHADE, $\mu F = 0.8$, $\mu CR = 0.5$, $\mu FH = \mu CRH = 0.9$, $ps = 12 \cdot D \sim 4$, $p = 0.2 - 0.1$
jSO	$F, CR \& rrac$ same as iLSHADE, $\mu F = 0.3$, $\mu CR = 0.8$, $ps = 25 \cdot \ln D \cdot D \sim 4$, $p = 0.25 - 0.125$, $H = 5$
HARD-DE	$\mu F = 0.3$, $\mu CR = 0.8$, $F \& CR$ same as LSHADE, $p = 0.11$, $ps = 25 \cdot lnD \cdot D \sim 4$, $rrac, A = 1.6$, $rrac, B = 3$, $k = 4$
HPDE	$\mu F = \mu CR = 0.5$, $rrac = 1.6$, $psini = 18 \cdot D$, $p\min = 4$, $n = 2 \cdot D$, $\xi = 0.001$, $H = 5$, $p = 0.2 - 0.05$

TABLE 2 | Characteristics of 12 PEMFCs used in this work.

Sl. no.	PEMFC type	Power (W)	Ncells (no)	A (cm^2)	l (μm)	T (K)	J_{max} (mA/cm^2)	PH_2 (bar)	PO_2 (bar)
FC1	BCS 500 W	500	32	64	178	333	469	1.0	0.2095
FC2	NetStack PS6	6000	65	240	178	343	1125	1.0	1.0
FC3	SR-12	500	48	62.5	25	323	672	1.47628	0.2095
FC4	H-12-1	12	13	8.1	25	323	246.9	0.4935	1.0
FC 5	Ballard Mark V	5000	35	232	178	343	1500	1.0	1.0
FC 6	STD-1	250	24	27	127	343	860	1.0	1.0
FC 7	Horizon	500	36	52	25	338	446	0.55	1.0
FC8	STD-2	250	24	27	127	343	860	1.5	1.5
FC9	STD-3	250	24	27	127	343	860	2.5	3.0
FC10	STD-4	250	24	27	127	353	860	2.5	3.0
FC11	H-12-2	12	13	8.1	25	302	246.9	0.4	1.0
FC12	H-12-3	13	13	8.1	25	312	246.9	0.5	1.0

TABLE 3 | Parameters estimated for FC1.

Algorithm	E-QUATRE	iLSHADE	CRADE	L-SHADE	jSO	HARD-DE	LSHADE-cnEpSin	DE	PCM-DE	HPDE
ξ_1	−0.9840126	−1.1770707	−0.8532	−0.8710833	−1.1564251	−0.9553534	−1.0713703	−1.0620494	−1.1975945	−0.9919514
ξ_2	0.00301	0.0032509	0.0030794	0.002331	0.0033698	0.0025771	0.0035716	0.0031181	0.0037194	0.0026047
ξ_3	6.454E−05	4.233E−05	9.387E−05	4.229E−05	5.396E−05	4.176E−05	8.338E−05	5.6E−05	6.911E−05	3.65E−05
ξ_4	−0.0001814	−0.0001919	−0.0001929	−0.0001921	−0.000193	−0.0001935	−0.0001928	−0.0001929	−0.0001787	−0.000193
λ	20.681348	20.167951	23	21.588182	20.888681	21.555674	21.468502	20.820627	17.286624	20.877244
R_c	0.0007508	0.0001198	0.0002816	0.0002173	0.0001051	0.0001573	0.0001644	0.0001016	0.0003703	0.0001
B	0.0136	0.0155994	0.0162647	0.0159267	0.0161076	0.0159731	0.0161855	0.0160809	0.0136	0.0161261
Min.	0.0550084	0.0261388	0.0256558	0.0259422	0.0255046	0.0261796	0.0256142	0.0254995	0.0665078	0.0254927
Max.	0.1924899	0.0319448	0.085535	0.0333606	0.025796	0.0499675	0.0261432	0.025561	0.1757013	0.0254927
Mean	0.1133755	0.0281778	0.0468485	0.0292157	0.0256313	0.0335568	0.0258695	0.0255143	0.1251737	0.0254927
Std.	0.053443	0.0024462	0.0226263	0.0036953	0.0001194	0.0099976	0.0001972	2.616E−05	0.045335	7.42E−09
RT	4.2058874	6.7180226	3.1583165	3.0451559	6.187678	4.541507	3.5360303	4.4975652	6.0141956	0.3451812
FR	9.2	5.8	7.4	6.4	3	6.6	4	2.2	9.4	1

its reliability, whereas other algorithms exhibit higher maximum values, such as PCM-DE at 0.414214 and E-QUATRE at 0.5139. The mean value for HPDE is the lowest at 0.275211, underscoring its efficiency and stability across multiple runs, outperforming others like E-QUATRE with a mean of 0.355667 and DE with 0.287025. The standard deviation of HPDE is 1.44E−16, showcasing unparalleled consistency, while other algorithms like PCM-DE and E-QUATRE show higher variability with std. values of 0.055274 and 0.100594, respectively. In terms of runtime, HPDE is significantly faster with an RT of 0.081078 s, outperforming all other algorithms with the next closest being CRADE at 3.551627 s. The Friedman Rank further highlights HPDE's dominance with a rank of 1, indicating the best overall performance among the evaluated algorithms. In comparison, other algorithms like PCM-DE and E-QUATRE have much higher Friedman Ranks of 9.2 and 7.8, respectively. In Tables 5 and 6, HDPE not only consistently outperforms other algorithms in terms of key metrics but also demonstrates unparalleled stability and efficiency, making it the most effective algorithm in this evaluation shown in Figure 2.

In Table 7, HPDE demonstrates superior performance with a minimum value of 0.242284, indicating its efficiency relative to other algorithms like E-QUATRE, iLSHADE, CRADE, L-SHADE, jSO, HARD-DE, LSHADE-cnEpSin, DE, and PCM-DE on FC2. The maximum value for HPDE remains consistent at 0.242927, highlighting its reliability, whereas other algorithms show higher maximum values, with PCM-DE reaching 0.430216 and E-QUATRE at 0.816536. The mean value for HPDE is the lowest at 0.24267, underscoring its effectiveness and stability across multiple runs, outperforming others like E-QUATRE with a mean of 0.458016 and DE at 0.242358. The standard deviation of HPDE is 0.000352, showcasing exceptional consistency, while other algorithms, such as E-QUATRE and PCM-DE, exhibit higher variability with std. values of 0.221732 and 0.078617, respectively. In terms of runtime, HPDE is significantly faster with an RT of 0.055785 s, outperforming all other algorithms, with the next closest being CRADE at 2.485698 s. The Friedman Rank further highlights HPDE's dominance with a rank of 3.2, indicating strong overall performance among the evaluated algorithms. In comparison, other algorithms like PCM-DE

TABLE 4 | Performance metrics of HPDE algorithm for FC1.

Sl. No.	I_{exp} (A)	V_{exp} (V)	V_{est} (V)	P_{exp} (W)	P_{est} (W)	AE_v (A)	RE (%)	MBE
1	0.6	29	28.997221	17.4	17.398332	0.0027792	0.0095836	4.291E−07
2	2.1	26.31	26.305939	55.251	55.242472	0.004061	0.0154352	9.162E−07
3	3.58	25.09	25.093559	89.8222	89.834942	0.0035591	0.0141853	7.037E−07
4	5.08	24.25	24.254625	123.19	123.2135	0.0046254	0.0190738	1.189E−06
5	7.17	23.37	23.375422	167.5629	167.60178	0.0054224	0.0232024	1.633E−06
6	9.55	22.57	22.584622	215.5435	215.68314	0.0146224	0.0647867	1.188E−05
7	11.35	22.06	22.071335	250.381	250.50966	0.0113354	0.0513844	7.138E−06
8	12.54	21.75	21.758472	272.745	272.85124	0.0084718	0.038951	3.987E−06
9	13.73	21.45	21.461271	294.5085	294.66325	0.0112712	0.0525466	7.058E−06
10	15.73	21.09	20.987751	331.7457	330.13732	0.1022493	0.4848236	0.0005808
11	17.02	20.68	20.694519	351.9736	352.22071	0.0145189	0.0702073	1.171E−05
12	19.11	20.22	20.230996	386.4042	386.61433	0.0109959	0.0543812	6.717E−06
13	21.2	19.76	19.770954	418.912	419.14422	0.0109535	0.0554329	6.666E−06
14	23	19.36	19.366035	445.28	445.41881	0.0060353	0.031174	2.024E−06
15	25.08	18.86	18.866477	473.0088	473.17125	0.0064772	0.0343434	2.331E−06
16	27.17	18.27	18.274732	496.3959	496.52446	0.0047317	0.0258988	1.244E−06
17	28.06	17.95	17.953322	503.677	503.77022	0.003322	0.0185071	6.131E−07
18	29.26	17.3	17.292888	506.198	505.98991	0.0071118	0.0411085	2.81E−06
Average value						0.0129191	0.0613903	3.61E−05

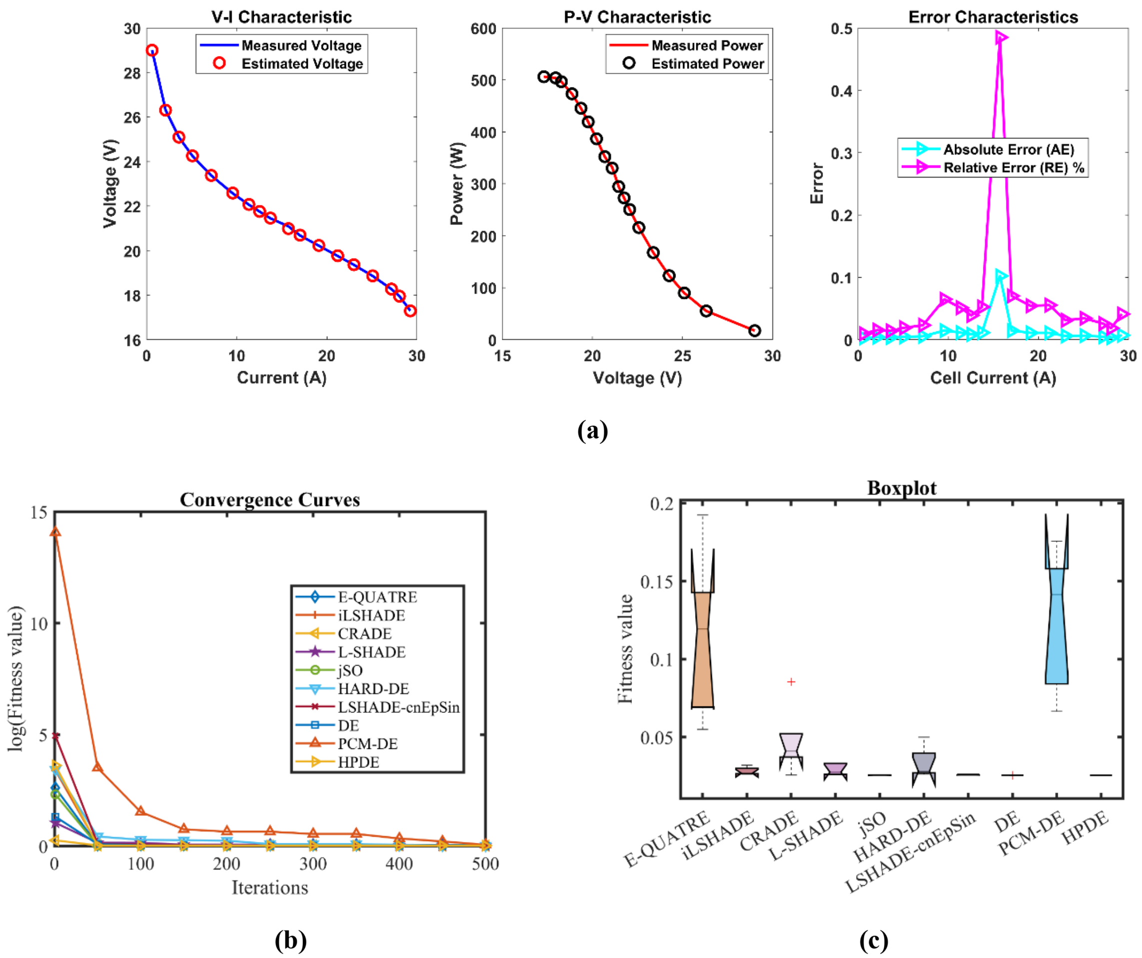

FIGURE 1 | HPDE algorithm characteristic curves of FC1: (a) $V-I$, $P-V$, and error curve; (b) convergence curve; and (c) box plot.

TABLE 5 | Parameters estimated for FC2.

Algorithm	E-QUATRE	iLSHADE	CRADE	L-SHADE	jSO	HARD-DE	LSHADE-cnEpSin	DE	PCM-DE	HPDE
ξ_1	−0.92873	−0.94569	−0.8532	−0.85929	−1.00202	−1.06121	−1.15198	−1.04589	−1.09404	−0.98321
ξ_2	0.003022	0.00296	0.003266	0.002822	0.002954	0.003576	0.003991	0.003013	0.003933	0.003221
ξ_3	6.48E−05	5.69E−05	0.000098	6.5E−05	4.47E−05	7.68E−05	8.76E−05	3.96E−05	9.55E−05	6.76E−05
ξ_4	−9.5E−05	−9.5E−05	−9.5E−05	−9.5E−05	−9.5E−05	−9.5E−05	−9.5E−05	−9.5E−05	−9.5E−05	−9.5E−05
λ	14	14	14	14	14.00912	14	14	14.15152	15.06894	14
R_c	0.000122	0.000109	0.0001	0.000115	0.000114	0.000114	0.00011	0.000144	0.0001	0.00012
B	0.016118	0.018416	0.019593	0.017632	0.017895	0.01758	0.017726	0.015808	0.029847	0.016788
Min.	0.275635	0.275436	0.2759	0.275302	0.275408	0.275359	0.275886	0.277689	0.285484	0.275211
Max.	0.5139	0.291685	0.276061	0.321702	0.280392	0.281342	0.280165	0.293302	0.414214	0.275211
Mean	0.355667	0.279778	0.275996	0.291059	0.277505	0.277454	0.276858	0.287025	0.342327	0.275211
Std.	0.100594	0.00696	8.8E−05	0.021765	0.002328	0.002424	0.001856	0.006797	0.055274	1.44E−16
RT	4.210993	4.207103	3.551627	3.723225	7.769565	4.103148	4.110283	4.804308	8.454202	0.081078
FR	7.8	4.4	4.2	5.6	4.6	5.2	5.2	7.8	9.2	1

and E-QUATRE have higher Friedman Ranks of 9.4 and 9.6, respectively. In Tables 7 and 8, overall, HDPE not only consistently excels in performance across all metrics but also demonstrates superior stability and efficiency, establishing it as the top-performing algorithm in this evaluation shown in Figure 3.

In Table 9, HPDE demonstrates superior performance with a minimum value of 0.1029149, which is identical to the best-performing algorithms such as E-QUATRE, iLSHADE, and CRADE. The maximum value for HPDE remains consistent at 0.1029149, indicating its stability, whereas other algorithms show higher maximum values, with PCM-DE reaching 0.1071709 and HARD-DE at 0.1046349. The mean value for HPDE is the lowest at 0.1029149, underscoring its effectiveness and stability across multiple runs, outperforming others like E-QUATRE with a mean of 0.1040502 and HARD-DE at 0.1036719. The standard deviation of HPDE is 7.28E−17, showcasing exceptional consistency, while other algorithms, such as E-QUATRE and PCM-DE, exhibit higher variability with std. values of 0.002532 and 0.0012265, respectively. In terms of runtime, HPDE has an RT of 5.9580159 s, which, while not the fastest, still indicates a balance between speed and performance. The Friedman Rank further highlights HPDE's dominance with a rank of 1.2, indicating strong overall performance among the evaluated algorithms. In comparison, other algorithms like PCM-DE and E-QUATRE have higher Friedman Ranks of 9.8 and 5, respectively. In Tables 9 and 10, overall, HDPE not only consistently excels in performance across all metrics but also demonstrates superior stability and efficiency, establishing it as the top-performing algorithm in this evaluation shown in Figure 4.

In Table 11, HPDE demonstrates superior performance with a minimum value of 0.1486318, which is equal to CRADE and the lowest among all algorithms, indicating its optimal performance. The maximum value for HPDE is also 0.1486318, showing its consistent performance, whereas other algorithms like E-QUATRE and HARD-DE have higher maximum values of 0.1704443 and 0.1572388, respectively. The mean value for HPDE is the lowest at 0.1486318, outperforming other algorithms such as E-QUATRE (0.1575585) and HARD-DE (0.1515186). The standard deviation of HPDE is exceptionally low at 1.54E−16, indicating outstanding stability, while other algorithms like E-QUATRE and PCM-DE exhibit higher variability with standard deviations of 0.0085177 and 0.0102698, respectively. In terms of runtime, HPDE has an RT of 0.0531358 s, significantly faster than others, like jSO (5.0872862) and PCM-DE (5.4723894). The Friedman Rank further highlights HPDE's dominance with a rank of 1, indicating the best overall performance among the evaluated algorithms. In comparison, other algorithms like PCM-DE and E-QUATRE have higher Friedman Ranks of 9.8 and 8.6, respectively. In Tables 11 and 12, overall, HDPE not only consistently excels in performance across all metrics but also demonstrates superior stability and efficiency, establishing it as the top-performing algorithm in this evaluation shown in Figure 5.

In Table 13, HPDE demonstrates superior performance with a minimum value of 0.2837738, which is equal to CRADE and the lowest among all algorithms, indicating its optimal performance. The maximum value for HPDE is also 0.2837738, showing its consistent performance, whereas other algorithms like E-QUATRE and HARD-DE have higher maximum values of 0.3639893 and 0.3412907, respectively. The mean value for HPDE is the lowest at 0.2837738, outperforming other algorithms such as E-QUATRE (0.329312) and HARD-DE (0.3166119). The standard deviation of HPDE is exceptionally low at 1.90E−15, indicating outstanding stability, while other algorithms like E-QUATRE and PCM-DE exhibit higher variability with standard deviations of 0.0209551 and 0.0357153, respectively. In terms of runtime, HPDE has an RT of 0.0466722 s, significantly faster than others like jSO (4.7808585) and PCM-DE (5.0206069). The Friedman Rank further highlights HPDE's dominance with a rank of 1.2, indicating the best overall performance among the evaluated algorithms. In comparison, other algorithms like PCM-DE and E-QUATRE have higher Friedman Ranks of 9.2 and 9, respectively. In Tables 13 and 14, HDPE not only consistently outperforms other algorithms in terms of key metrics but also demonstrates unparalleled stability and efficiency, making it the most effective algorithm in this evaluation shown in Figure 6.

In Table 15, HPDE demonstrates superior performance with a minimum value of 0.1217552, which is among the lowest and

TABLE 6 | Performance metrics of HPDE algorithm for FC2.

Sl. No.	I_{exp} (A)	V_{exp} (V)	V_{est} (V)	P_{exp} (W)	P_{est} (W)	AE_v (A)	RE (%)	MBE
1	2.25	61.64	62.327092	138.69	140.23596	0.6870919	1.1146851	0.0162791
2	6.75	59.57	59.753914	402.0975	403.33892	0.1839142	0.3087363	0.0011664
3	9	58.94	59.023004	530.46	531.20703	0.0830036	0.1408272	0.0002376
4	15.75	57.54	57.472456	906.255	905.19118	0.0675438	0.1173859	0.0001573
5	20.25	56.8	56.695015	1150.2	1148.0741	0.104985	0.1848327	0.0003801
6	24.75	56.13	56.023046	1389.2175	1386.5704	0.1069536	0.1905462	0.0003945
7	31.5	55.23	55.138042	1739.745	1736.8483	0.0919577	0.1664995	0.0002916
8	36	54.66	54.603002	1967.76	1965.7081	0.0569979	0.1042772	0.000112
9	45	53.61	53.618873	2412.45	2412.8493	0.0088727	0.0165504	2.715E−06
10	51.75	52.86	52.932653	2735.505	2739.2648	0.0726529	0.137444	0.000182
11	67.5	51.91	51.435596	3503.925	3471.9027	0.4744041	0.9138973	0.0077607
12	72	51.22	51.025403	3687.84	3673.829	0.1945965	0.3799229	0.0013058
13	90	49.66	49.426727	4469.4	4448.4054	0.2332729	0.46974	0.0018764
14	99	49	48.641017	4851	4815.4607	0.358983	0.7326184	0.0044438
15	105.8	48.15	48.049174	5094.27	5083.6026	0.1008264	0.2094007	0.0003506
16	110.3	47.52	47.657407	5241.456	5256.612	0.1374069	0.289156	0.0006511
17	117	47.1	47.07284	5510.7	5507.5223	0.0271597	0.057664	2.544E−05
18	126	46.48	46.283068	5856.48	5831.6666	0.1969318	0.4236915	0.0013373
19	135	45.66	45.485315	6164.1	6140.5175	0.1746853	0.3825785	0.0010522
20	141.8	44.85	44.87552	6359.73	6363.3488	0.0255201	0.056901	2.246E−05
21	150.8	44.24	44.056854	6671.392	6643.7736	0.1831458	0.4139823	0.0011566
22	162	42.45	43.015703	6876.9	6968.5439	0.5657031	1.332634	0.0110352
23	171	41.66	42.157521	7123.86	7208.9361	0.4975213	1.1942422	0.0085354
24	182.3	40.68	41.047518	7415.964	7482.9625	0.367518	0.9034367	0.0046576
25	189	40.09	40.36955	7577.01	7629.8449	0.2795497	0.6973052	0.0026948
26	195.8	39.51	39.664139	7736.058	7766.2385	0.1541394	0.3901275	0.0008193
27	204.8	38.73	38.699845	7931.904	7925.7282	0.0301554	0.0778606	3.136E−05
28	211.5	38.15	37.955784	8068.725	8027.6484	0.1942156	0.5090842	0.0013007
29	220.5	37.38	36.914222	8242.29	8139.586	0.4657779	1.2460619	0.007481
Average value						0.2112237	0.4538652	0.0026118

equal to CRADE and jSO, indicating its optimal performance. The maximum value for HPDE is also 0.1217552, showing its consistent performance, whereas other algorithms like PCM-DE have a higher maximum value of 0.3534266. The mean value for HPDE is the lowest at 0.1217552, outperforming other algorithms such as E-QUATRE (0.1327644) and HARD-DE (0.1253692). The standard deviation of HPDE is exceptionally low at 1.90E−16, indicating outstanding stability, while other algorithms like E-QUATRE and PCM-DE exhibit higher variability with standard deviations of 0.0088173 and 0.0859484, respectively. In terms of runtime, HPDE has an RT of 0.0514466 s, significantly faster than others like jSO (5.078283) and PCM-DE (5.3436805). The Friedman Rank further highlights HPDE's dominance with a rank of 1.2, indicating the best overall performance among the evaluated algorithms. In comparison, other algorithms like PCM-DE and E-QUATRE have higher Friedman Ranks of 10 and 8.2, respectively. In Tables 15 and 16, HDPE not only consistently outperforms other algorithms in terms of key metrics but also demonstrates unparalleled stability and efficiency, making it the most effective algorithm in this evaluation shown in Figure 7.

In Table 17, HPDE demonstrates exceptional performance with a minimum value of 0.0784922, which is among the lowest and equal to CRADE and jSO, indicating its optimal performance. The maximum value for HPDE is also 0.0784922, showing its consistent performance, whereas other algorithms like PCM-DE have a

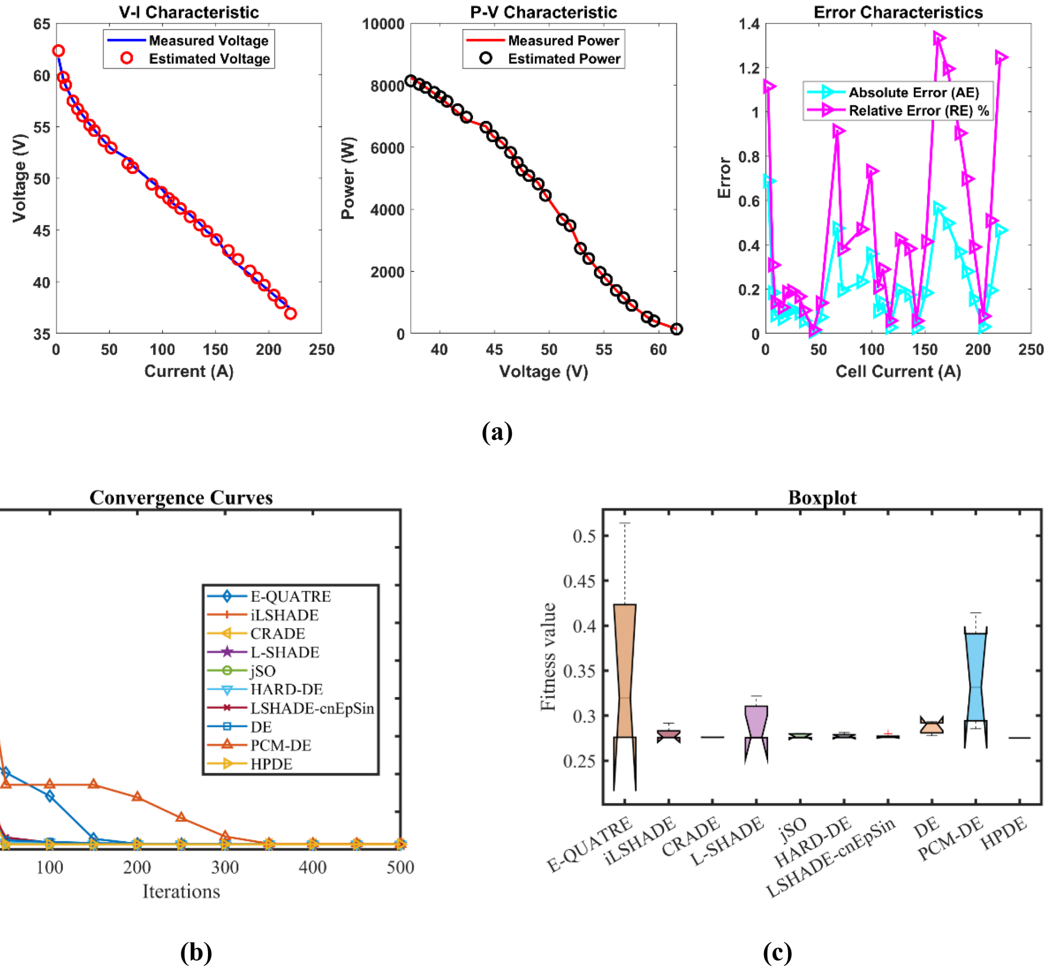

FIGURE 2 | HPDE algorithm characteristic curves of FC2: (a) $V-I$, $P-V$, and error curve; (b) convergence curve; and (c) box plot.

TABLE 7 | Parameters estimated for FC3.

Algorithm	E-QUATRE	iLSHADE	CRADE	L-SHADE	jSO	HARD-DE	LSHADE-cnEpSin	DE	PCM-DE	HPDE
ξ_1	−0.8532	−1.1548	−1.19969	−1.17578	−1.16414	−1.11316	−0.89661	−1.05089	−1.10717	−0.85428
ξ_2	0.002476	0.004168	0.003361	0.003851	0.004093	0.003881	0.003079	0.003099	0.003151	0.002547
ξ_3	4.82E−05	9.7E−05	0.000036	7.25E−05	9.04E−05	8.69E−05	7.83E−05	4.88E−05	3.96E−05	5.25E−05
ξ_4	−9.5E−05	−9.5E−05	−9.5E−05	−9.6E−05	−9.5E−05	−9.9E−05	−9.6E−05	−9.5E−05	−0.00011	−9.5E−05
λ	23	22.8281	23	20.15961	21.86346	14.07505	22.61901	22.99561	17.25396	23
R_c	0.0001	0.000791	0.000673	0.000491	0.000637	0.000168	0.00068	0.000684	0.000756	0.000673
B	0.190188	0.172922	0.17532	0.177894	0.175624	0.179236	0.174983	0.175127	0.165187	0.17532
Min.	0.265118	0.242674	0.242284	0.242924	0.242352	0.244854	0.242443	0.242297	0.272107	0.242284
Max.	0.816536	0.245288	0.247458	0.24375	0.242842	0.24703	0.242661	0.242422	0.430216	0.242927
Mean	0.458016	0.244326	0.245948	0.243256	0.242608	0.245864	0.242543	0.242358	0.351472	0.24267
Std.	0.221732	0.001177	0.002292	0.000364	0.000175	0.000854	8.18E−05	5.18E−05	0.078617	0.000352
RT	3.125907	2.975387	2.485698	2.638388	5.822444	2.971708	3.161894	3.5453	6.12894	0.055785
FR	9.6	6	6.6	5.2	3.2	7.2	3	1.6	9.4	3.2

higher maximum value of 0.2378285. The mean value for HPDE is the lowest at 0.0784922, outperforming other algorithms such as E-QUATRE (0.087973) and HARD-DE (0.0799228). The standard deviation of HPDE is exceptionally low at 3.67E−16, indicating outstanding stability, while other algorithms like E-QUATRE and PCM-DE exhibit higher variability with standard deviations of 0.0114463 and 0.0422313, respectively. In terms of runtime, HPDE has an RT of 0.0499442 s, significantly faster than others, like jSO (5.1180527) and PCM-DE (5.48773). The Friedman Rank further highlights HPDE's dominance with a rank of 1, indicating

TABLE 8 | Performance metrics of HPDE algorithm for FC3.

Sl. No.	I_{exp} (A)	V_{exp} (V)	V_{est} (V)	P_{exp} (W)	P_{est} (W)	AE_v (A)	RE (%)	MBE
1	1.004	43.17	43.340807	43.34268	43.51417	0.1708071	0.3956615	0.0016208
2	3.166	41.14	41.090075	130.24924	130.09118	0.0499245	0.1213527	0.0001385
3	5.019	40.09	39.91451	201.21171	200.33092	0.1754902	0.4377406	0.0017109
4	7.027	39.04	38.85715	274.33408	273.04919	0.1828501	0.4683662	0.0018575
5	8.958	37.99	37.933462	340.31442	339.80796	0.0565376	0.1488224	0.0001776
6	10.97	37.08	37.014534	406.7676	406.04944	0.0654656	0.1765524	0.0002381
7	13.05	36.03	36.079903	470.1915	470.84274	0.0499032	0.1385045	0.0001384
8	15.06	35.19	35.171362	529.9614	529.6807	0.0186385	0.0529653	1.93E−05
9	17.07	34.07	34.242086	581.5749	584.51241	0.1720858	0.5050949	0.0016452
10	19.07	33.02	33.283123	629.6914	634.70916	0.2631235	0.7968609	0.0038463
11	21.08	32.04	32.270698	675.4032	680.26631	0.2306976	0.7200301	0.0029567
12	23.01	31.2	31.237691	717.912	718.77927	0.037691	0.1208046	7.892E−05
13	24.94	29.8	30.127369	743.212	751.37658	0.3273689	1.0985532	0.0059539
14	26.87	28.96	28.917131	778.1552	777.00332	0.0428688	0.1480275	0.0001021
15	28.96	28.12	27.457754	814.3552	795.17656	0.662246	2.355071	0.024365
16	30.81	26.3	25.991802	810.303	800.80741	0.3081983	1.1718566	0.005277
17	32.97	24.06	23.984866	793.2582	790.78104	0.0751339	0.3122772	0.0003136
18	34.9	21.4	21.785631	746.86	760.31852	0.385631	1.802014	0.0082617
Average value						0.1819256	0.6094753	0.0032612

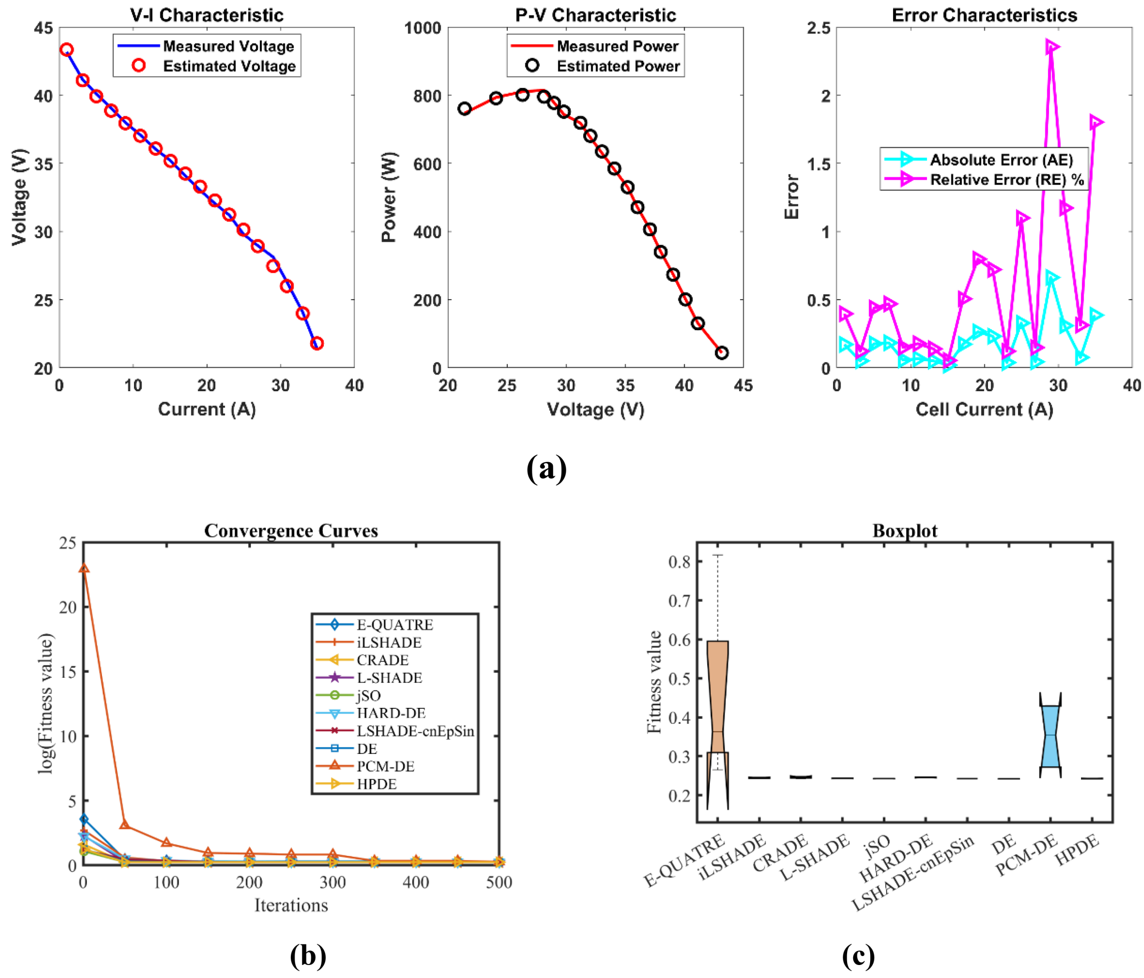

FIGURE 3 | HPDE algorithm characteristic curves of FC3: (a) $V-I$, $P-V$, and error curve, (b) convergence curve, and (c) and box plot.

TABLE 9 | Parameters estimated for FC4.

Algorithm	E-QUATRE	iLSHADE	CRADE	L-SHADE	jSO	HARD-DE	LSHADE-cnEpSin	DE	PCM-DE	HPDE
ξ_1	−0.9521623	−0.9033323	−0.8532	−1.0910036	−1.0900792	−1.0303207	−1.0723444	−1.0358307	−1.0224857	−0.8532266
ξ_2	0.0018149	0.0023758	0.0015086	0.0027994	0.0028216	0.0027047	0.0027063	0.0023836	0.0023385	0.002092
ξ_3	0.000036	8.713E−05	0.000036	7.583E−05	7.762E−05	8.252E−05	7.329E−05	5.824E−05	5.815E−05	7.789E−05
ξ_4	−0.0001113	−0.0001113	−0.0001113	−0.0001117	−0.0001113	−0.0001112	−0.0001113	−0.0001113	−0.0001144	−0.0001113
λ	14	14	14	14	14.000492	14	14	14.002416	14.255044	14
R_c	0.0008	0.0008	0.0008	0.0006482	0.0007994	0.0006708	0.0008	0.0007999	0.0002325	0.0008
B	0.0136	0.0136	0.0136	0.0136852	0.013601	0.0137737	0.0136	0.0136001	0.0136	0.0136
Min.	0.1029149	0.1029149	0.1029149	0.1030905	0.102916	0.1030858	0.102915	0.1029159	0.1037461	0.1029149
Max.	0.1085796	0.1035542	0.1036409	0.1041188	0.1034497	0.1046349	0.1029183	0.1029224	0.1071709	0.1029149
Mean	0.1040502	0.1031311	0.1032053	0.1034761	0.1030435	0.1036719	0.102916	0.1029178	0.1052594	0.1029149
Std.	0.002532	0.0002963	0.0003977	0.0004294	0.000231	0.0005938	1.348E−06	2.661E−06	0.0012265	7.278E−17
RT	3.1941279	3.068342	2.5516256	2.6593313	5.5792584	2.9741345	2.9298123	3.5510224	0.0552545	5.9580159
FR	5	5.4	4	7.4	5.6	8.2	3.8	4.6	9.8	1.2

TABLE 10 | Performance metrics of HPDE algorithm for FC4.

Sl. No.	I_{exp} (A)	V_{exp} (V)	V_{est} (V)	P_{exp} (W)	P_{est} (W)	AE_v (A)	RE (%)	MBE
1	0.104	9.58	9.755528	0.99632	1.014575	0.175528	1.832238	0.001712
2	0.2	9.42	9.435532	1.884	1.887106	0.015532	0.164879	1.34E−05
3	0.309	9.25	9.215304	2.85825	2.847529	0.034696	0.375097	6.69E−05
4	0.403	9.2	9.075993	3.7076	3.657625	0.124007	1.347904	0.000854
5	0.51	9.09	8.94789	4.6359	4.563424	0.14211	1.563361	0.001122
6	0.614	8.95	8.842713	5.4953	5.429426	0.107287	1.198742	0.000639
7	0.703	8.85	8.762859	6.22155	6.16029	0.087141	0.984639	0.000422
8	0.806	8.74	8.678684	7.04444	6.995019	0.061316	0.70156	0.000209
9	0.908	8.65	8.601586	7.8542	7.81024	0.048414	0.559702	0.00013
10	1.076	8.45	8.483392	9.0922	9.12813	0.033392	0.395172	6.19E−05
11	1.127	8.41	8.448866	9.47807	9.521872	0.038866	0.462138	8.39E−05
12	1.288	8.2	8.341383	10.5616	10.7437	0.141383	1.724177	0.001111
13	1.39	8.12	8.272661	11.2868	11.499	0.152661	1.880064	0.001295
14	1.45	8.11	8.231197	11.7595	11.93524	0.121197	1.494416	0.000816
15	1.578	8.05	8.137513	12.7029	12.841	0.087513	1.087123	0.000425
16	1.707	7.99	8.028855	13.63893	13.70525	0.038855	0.486291	8.39E−05
17	1.815	7.95	7.912601	14.42925	14.36137	0.037399	0.470424	7.77E−05
18	1.9	7.94	7.777412	15.086	14.77708	0.162588	2.04771	0.001469
						0.089438	1.043091	0.000588

the best overall performance among the evaluated algorithms. In comparison, other algorithms like PCM-DE and E-QUATRE have higher Friedman Ranks of 10 and 8.6, respectively. In Tables 17 and 18, HDPE not only consistently outperforms other algorithms in terms of key metrics but also demonstrates unparalleled stability and efficiency, making it the most effective algorithm in this evaluation shown in Figure 8.

In Table 19, HPDE shows exceptional performance with a minimum value of 0.2023192, which is the lowest among all algorithms, indicating its optimal performance. The maximum value for HPDE is also the lowest at 0.2023192, demonstrating its consistent performance, while other algorithms like PCM-DE have a higher maximum value of 0.2594436. The mean value for HPDE is the lowest at 0.2023192, outperforming other algorithms such as E-QUATRE (0.2111907) and HARD-DE (0.2047157). The standard deviation of HPDE is the lowest at 3.63E−16, indicating exceptional stability, whereas other algorithms like E-QUATRE and PCM-DE exhibit higher variability with standard deviations of 0.0069429 and 0.0163137, respectively. In terms of runtime,

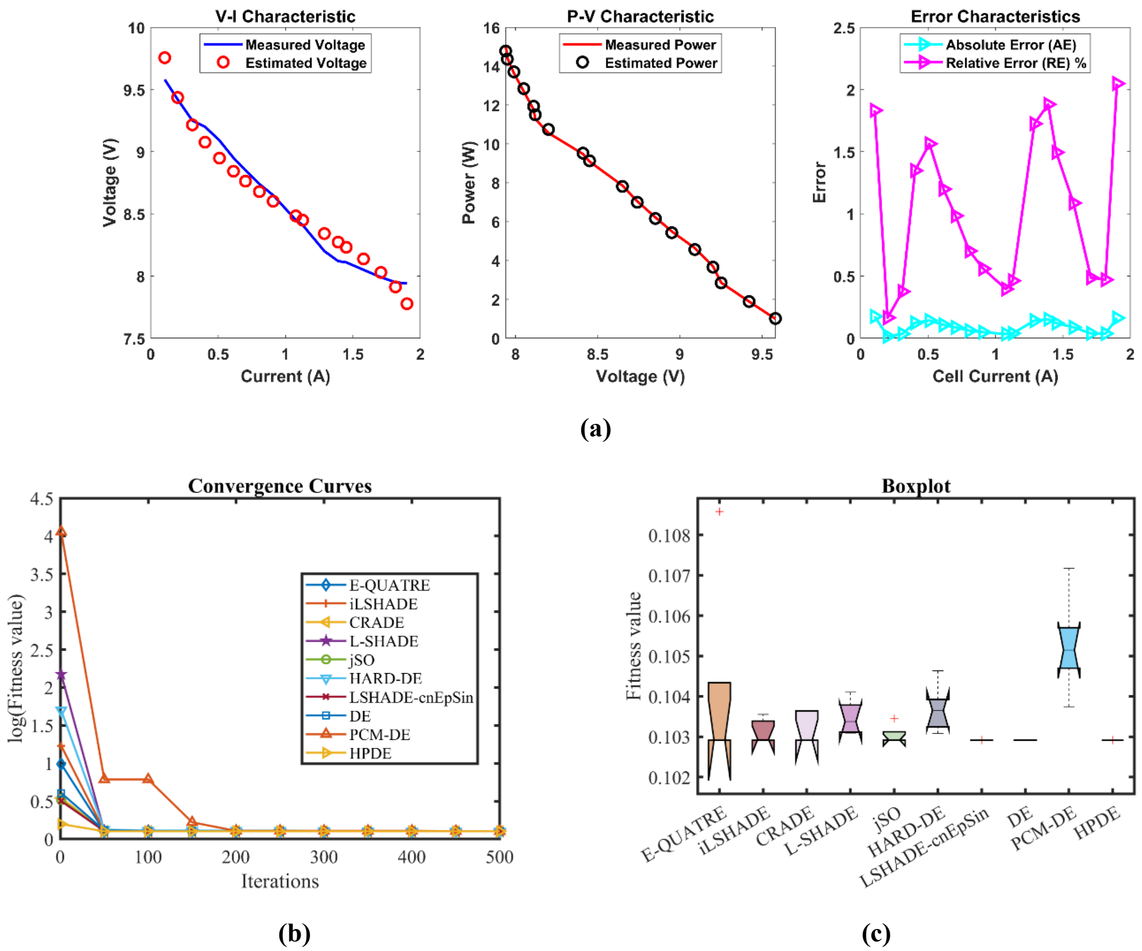

FIGURE 4 | HPDE algorithm characteristic curves of FC4: (a) $V-I$, $P-V$, and error curve; (b) convergence curve; and (c) box plot.

TABLE 11 | Parameters estimated for FC5.

Algorithm	E-QUATRE	iLSHADE	CRADE	L-SHADE	jSO	HARD-DE	LSHADE-cnEpSin	DE	PCM-DE	HPDE
ξ_1	−1.1685183	−0.928982	−0.8763104	−1.1959442	−0.8969871	−0.8911592	−0.9146127	−1.0328635	−1.1684013	−1.0153083
ξ_2	0.0039235	0.0026223	0.0031951	0.0036004	0.0024971	0.002545	0.0025231	0.0035207	0.0033949	0.0027314
ξ_3	8.915E−05	4.611E−05	0.000098	6.039E−05	4.386E−05	4.856E−05	4.209E−05	8.867E−05	5.095E−05	0.000036
ξ_4	−0.0001749	−0.0001735	−0.0001739	−0.0001749	−0.0001742	−0.0001731	−0.0001738	−0.0001742	−0.0001807	−0.0001739
λ	14.447742	15.988553	14.439089	14.973109	14.555931	14.468932	14.404147	14.514322	15.089291	14.439129
R_c	0.0001	0.0005922	0.0001	0.0001797	0.0001355	0.0001679	0.0001038	0.0001	0.0001344	0.0001
B	0.0136	0.0146946	0.0137949	0.0145473	0.0138162	0.0136332	0.0136	0.0139118	0.0136833	0.013795
Min.	0.1489332	0.1494602	0.1486318	0.1488948	0.1486985	0.1487643	0.1486828	0.1486404	0.1520748	0.1486318
Max.	0.1704443	0.1549261	0.1497299	0.1497091	0.1497913	0.1572388	0.1489934	0.1487031	0.1785777	0.1486318
Mean	0.1575585	0.1508911	0.148858	0.1491595	0.1490786	0.1515186	0.1488216	0.1486595	0.1633949	0.1486318
Std.	0.0085177	0.0023164	0.0004874	0.0003202	0.0005132	0.0034045	0.0001306	2.596E−05	0.0102698	1.539E−16
RT	2.8288384	2.6201253	2.2417895	2.4025326	5.0872862	2.7321435	2.6997915	3.1753678	5.4723894	0.0531358
FR	8.6	7.6	3	5.8	4.8	7	4.6	2.8	9.8	1

HPDE has the fastest RT at 0.0496575 s, significantly faster than others like jSO (5.0824901) and PCM-DE (5.4549681). The Friedman Rank further highlights HPDE's dominance with a rank of 1.1, indicating the best overall performance among the evaluated algorithms. In comparison, other algorithms like PCM-DE and E-QUATRE have higher Friedman Ranks of 10 and 8.4, respectively. In Tables 19 and 20, HDPE not only consistently outperforms other algorithms in terms of key metrics but also demonstrates unparalleled stability and efficiency, making it the most effective algorithm in this evaluation shown in Figure 9.

TABLE 12 | Performance metrics of HPDE algorithm for FC5.

Sl. No.	I_{exp} (A)	V_{exp} (V)	V_{est} (V)	P_{exp} (W)	P_{est} (W)	AE_v (A)	RE (%)	MBE
1	0.5	23.5	23.48308	11.75	11.74154	0.016916	0.071982	1.91E−05
2	2.1	21.5	21.2513	45.15	44.62774	0.248696	1.156726	0.004123
3	2.8	20.5	20.75982	57.4	58.12748	0.259815	1.267392	0.0045
4	4	19.9	20.10958	79.6	80.43831	0.209578	1.053157	0.002928
5	5.7	19.5	19.39753	111.15	110.5659	0.102466	0.525469	0.0007
6	7.1	19	18.90726	134.9	134.2415	0.092745	0.488129	0.000573
7	8	18.5	18.61964	148	148.9571	0.119642	0.646716	0.000954
8	11.1	17.8	17.72276	197.58	196.7226	0.077244	0.433955	0.000398
9	13.7	17.3	17.02409	237.01	233.2301	0.275909	1.594847	0.005075
10	16.5	16.2	16.27465	267.3	268.5317	0.074647	0.460782	0.000371
11	17.5	15.9	15.99828	278.25	279.97	0.098283	0.618135	0.000644
12	18.9	15.5	15.59366	292.95	294.7202	0.093661	0.604266	0.000585
13	20.3	15.1	15.15114	306.53	307.5682	0.051143	0.338696	0.000174
14	22	14.6	14.47819	321.2	318.5202	0.12181	0.834313	0.000989
15	22.9	13.8	13.82904	316.02	316.6851	0.029045	0.210469	5.62E−05
						0.124773	0.687002	0.001473

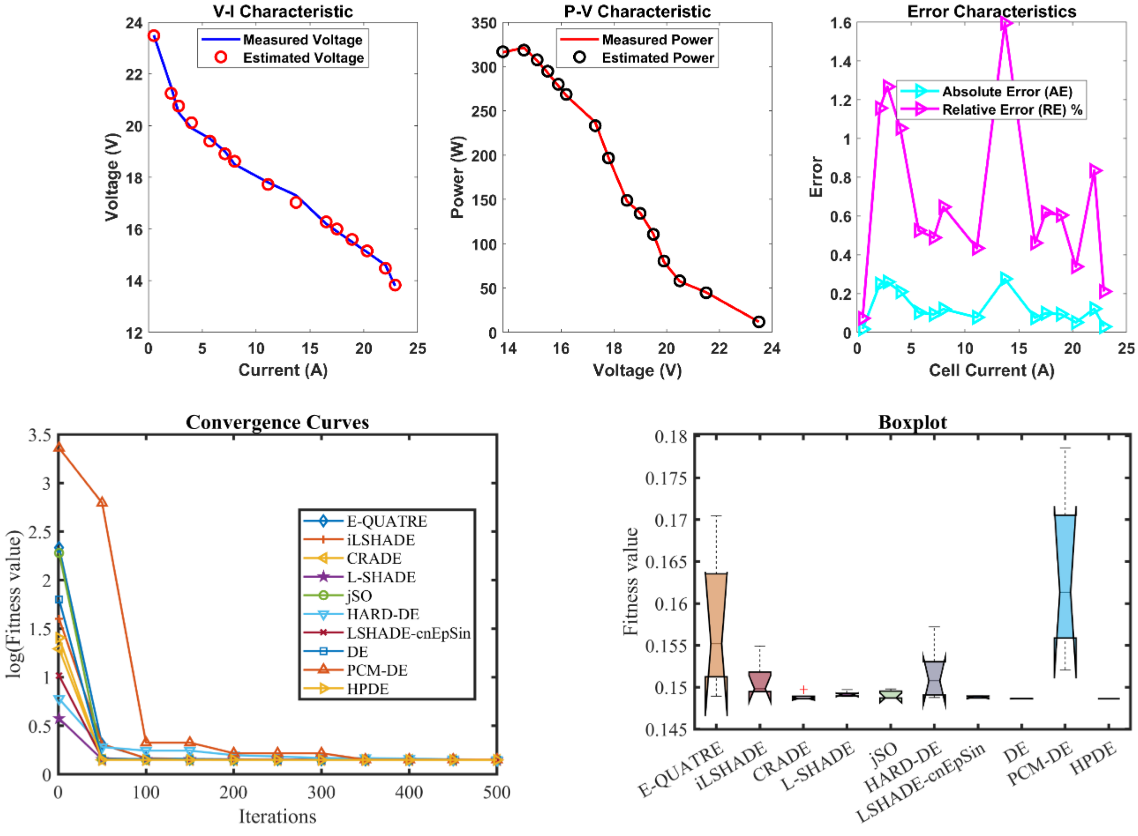

(b) **(c)**

FIGURE 5 | HPDE algorithm characteristic curves of FC5: (a) $V-I$, $P-V$, and error curve; (b) convergence curve; and (c) box plot.

In Table 21, HPDE demonstrates outstanding performance, with a minimum value of 0.1044462, which is the lowest among all algorithms, highlighting its optimal efficiency. The maximum value for HPDE is also the lowest at 0.1044462, underscoring its consistent and reliable performance, in contrast to other algorithms like PCM-DE, which have a significantly higher

TABLE 13 | Parameters estimated for FC6.

Algorithm	E-QUATRE	iLSHADE	CRADE	L-SHADE	jSO	HARD-DE	LSHADE-cnEpSin	DE	PCM-DE	HPDE
ξ_1	−1.19969	−0.8532	−0.8673845	−1.1625991	−1.0939508	−1.175682	−1.120507	−0.9327332	−0.9934473	−0.9864869
ξ_2	0.0031907	0.0026161	0.0027864	0.0030273	0.0032604	0.0031885	0.0032028	0.0026845	0.0026002	0.0022893
ξ_3	5.668E−05	8.883E−05	0.000098	5.269E−05	8.396E−05	6.141E−05	7.429E−05	7.689E−05	5.735E−05	3.73E−05
ξ_4	−0.000174	−0.0001697	−0.0001697	−0.0001707	−0.0001697	−0.0001726	−0.0001694	−0.0001697	−0.0001747	−0.0001697
λ	14	14	14	14	14.000026	19.254113	14	14.000511	14	14
R_c	0.0004324	0.0008	0.0008	0.0007998	0.0008	0.0007996	0.0008	0.0008	0.0006396	0.0008
B	0.0185327	0.0173175	0.0173175	0.0170399	0.0173153	0.0174668	0.0173495	0.0173168	0.0184819	0.0173175
Min.	0.3078982	0.2837738	0.2837738	0.2840087	0.2837741	0.2939847	0.2837923	0.2837807	0.3014926	0.2837738
Max.	0.3639893	0.3056855	0.3128681	0.3290755	0.2838289	0.3412907	0.2839161	0.2838515	0.3998247	0.2837738
Mean	0.329312	0.2882889	0.2951595	0.2976678	0.2837891	0.3166119	0.283832	0.2837978	0.3469956	0.2837738
Std.	0.0209551	0.0097292	0.0121004	0.0188761	2.282E−05	0.0204988	4.899E−05	3.011E−05	0.0357153	1.899E−15
RT	2.6561815	2.4680154	2.0804357	2.2105131	4.7808585	2.5588533	2.510228	3.184506	5.0206069	0.0466722
FR	9	4.4	4.8	6.6	3.4	7.8	4.6	4	9.2	1.2

TABLE 14 | Performance metrics of HPDE algorithm for FC6.

Sl. No.	I_{exp} (A)	V_{exp} (V)	V_{est} (V)	P_{exp} (W)	P_{est} (W)	AE_v (A)	RE (%)	MBE
1	0.6	29.37	29.7147	17.622	17.82882	0.344697	1.173637	0.00914
2	2.5	26.77739	26.62879	66.94348	66.57198	0.148596	0.554932	0.001699
3	5	25.29025	25.00559	126.4513	125.0279	0.284663	1.125584	0.006233
4	7.5	24.28186	23.96352	182.1139	179.7264	0.318338	1.311012	0.007795
5	10	23.418	23.14755	234.18	231.4755	0.270455	1.154901	0.005627
6	12	22.7391	22.57673	272.8692	270.9208	0.162373	0.71407	0.002028
7	14	22.05852	22.04306	308.8193	308.6028	0.015466	0.070114	1.84E−05
8	16	21.38615	21.52088	342.1784	344.3341	0.134735	0.630011	0.001396
9	18	20.72173	20.98016	372.9911	377.6428	0.25843	1.247143	0.005137
10	20	20.026	20.364	400.52	407.28	0.338	1.687807	0.008788
11	21	19.63635	19.98092	412.3634	419.5992	0.344566	1.754735	0.009133
12	22	19.19181	19.45678	422.2198	428.0492	0.264977	1.380677	0.005401
13	23	18.66363	18.17812	429.2635	418.0968	0.485507	2.601355	0.018132
						0.259293	1.185075	0.006194

maximum value of 0.1950521. The mean value for HPDE is the lowest at 0.1044462, outperforming other algorithms such as CRADE (0.1175799) and E-QUATRE (0.1086723). The standard deviation of HPDE is the lowest at 1.947E−16, indicating exceptional stability, whereas other algorithms like CRADE and PCM-DE show higher variability with standard deviations of 0.0156071 and 0.0318177, respectively. In terms of runtime, HPDE has the fastest RT at 0.0499261 s, significantly quicker than other algorithms like jSO (5.0056106) and PCM-DE (5.3801302). The Friedman Rank further underscores HPDE's superiority with a rank of 1, indicating the best overall performance among the evaluated algorithms. In comparison, other algorithms like PCM-DE and E-QUATRE have higher Friedman Ranks of 9.8 and 6, respectively. In Tables 21 and 22, HDPE not only consistently outperforms other algorithms in terms of key metrics but also demonstrates unparalleled stability and efficiency, making it the most effective algorithm in this evaluation shown in Figure 10.

In Table 23, HPDE demonstrates outstanding performance with a minimum value of 0.0754843, which is the same as the best-performing algorithms iLSHADE, CRADE, jSO, and LSHADE-cnEpSin, indicating its optimal efficiency. The maximum value for HPDE is also one of the lowest at 0.0761032, closely following iLSHADE, suggesting consistent and reliable performance. The mean value for HPDE is 0.0756081, which is competitive and better than several other algorithms, such as PCM-DE (0.0994453) and E-QUATRE (0.0779909). The standard deviation of HPDE is impressively low at 0.0002768, indicating exceptional stability, whereas other algorithms like PCM-DE show higher variability with a standard deviation of 0.0172328. In terms of runtime, HPDE has one of the fastest RTs at 0.048964 s, significantly quicker than other algorithms like jSO (4.9699461) and PCM-DE (5.2673452). The Friedman Rank further underscores HPDE's superior performance with a rank of 2.9, indicating excellent overall performance among the evaluated algorithms. In comparison, other algorithms like PCM-DE

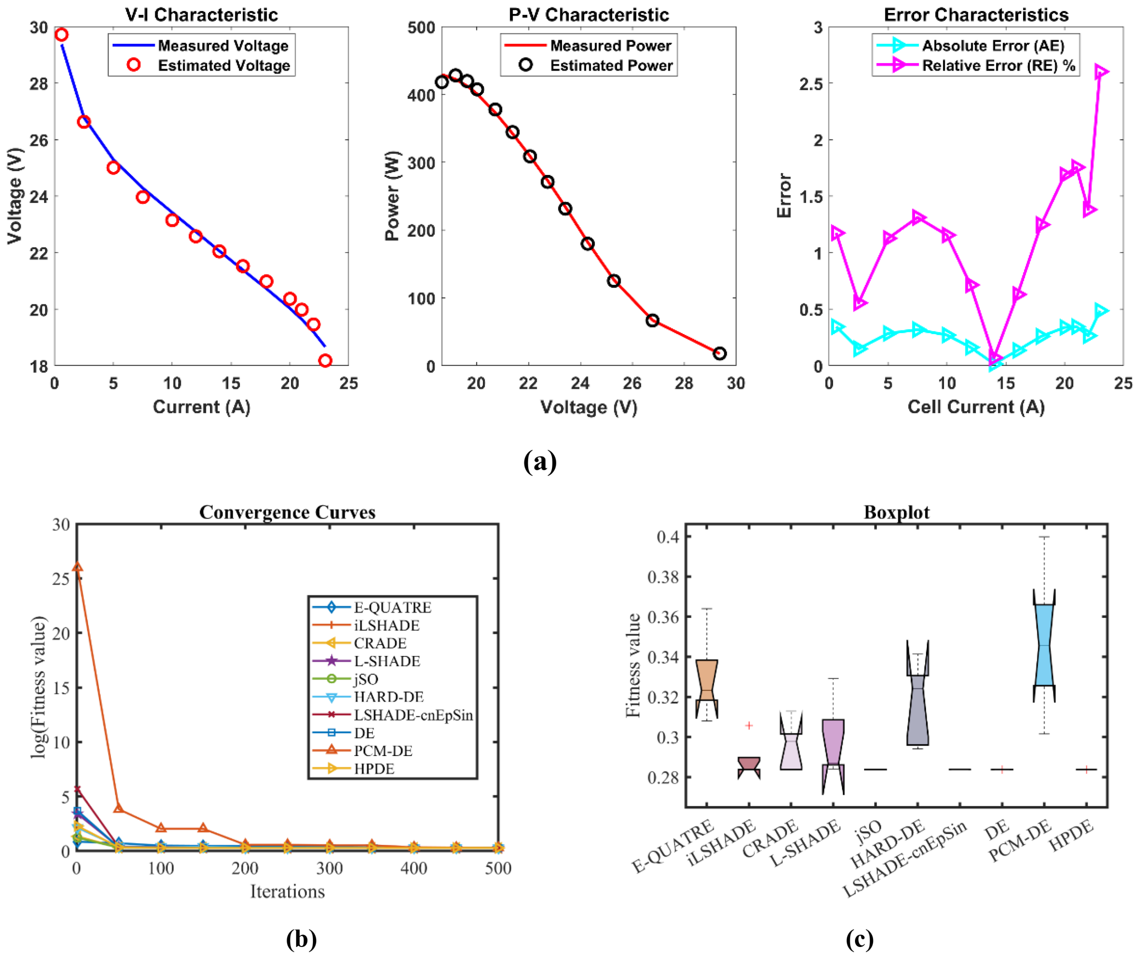

FIGURE 6 | HPDE algorithm characteristic curves of FC6: (a) $V-I$, $P-V$, and error curve; (b) convergence curve; and (c) box plot.

TABLE 15 | Parameters estimated for FC7.

Algorithm	E-QUATRE	iLSHADE	CRADE	L-SHADE	jSO	HARD-DE	LSHADE-cnEpSin	DE	PCM-DE	HPDE
ξ_1	−1.19969	−1.0196878	−1.19969	−0.9769334	−1.0394338	−0.8810538	−1.1402574	−1.0714187	−1.0040526	−0.9189721
ξ_2	0.0030764	0.0029442	0.0033489	0.002946	0.0031337	0.0028405	0.0033848	0.0029281	0.0024634	0.0026185
ξ_3	3.978E−05	6.885E−05	6.003E−05	7.814E−05	7.855E−05	9.096E−05	7.535E−05	5.658E−05	3.663E−05	6.65E−05
ξ_4	−0.0001519	−0.0001491	−0.0001493	−0.0001487	−0.0001493	−0.0001482	−0.0001493	−0.0001494	−0.0001419	−0.0001493
λ	22.980176	22.999999	23	23	23	23	22.952123	22.99982	19.338365	23
R_c	0.0001	0.0001133	0.0001	0.0001622	0.0001	0.0001882	0.0001	0.0001001	0.0003425	0.0001
B	0.0502815	0.0509285	0.0509795	0.0508328	0.0509795	0.0504517	0.051009	0.0509621	0.0478712	0.0509795
Min.	0.1234512	0.121919	0.1217552	0.122615	0.1217552	0.1232137	0.1218554	0.1217603	0.137449	0.1217552
Max.	0.1439856	0.1292771	0.1347178	0.1335755	0.1218322	0.1286454	0.1223814	0.1217913	0.3534266	0.1217552
Mean	0.1327644	0.1248954	0.1269402	0.1265548	0.1217772	0.1253692	0.1221106	0.1217704	0.2142682	0.1217552
Std.	0.0088173	0.0031768	0.0070999	0.004349	3.336E−05	0.0020689	0.0001916	1.311E−05	0.0859484	1.902E−16
RT	2.7923031	2.6525299	2.2224308	2.3808522	5.078283	2.728087	2.6928444	3.1766269	5.3436805	0.0514466
FR	8.2	6.2	4.4	7	3	7	4.8	3.2	10	1.2

and E-QUATRE have higher Friedman Ranks of 10 and 7.8, respectively. In Tables 23 and 24, HDPE not only consistently outperforms other algorithms in terms of key metrics but also demonstrates unparalleled stability and efficiency, making it the most effective algorithm in this evaluation shown in Figure 11.

In Table 25, HPDE demonstrates exceptional performance with a minimum value of 0.0641935, which is on par with the best-performing algorithms iLSHADE, CRADE, and LSHADE-cnEpSin, indicating its optimal efficiency. The maximum value for HPDE is also one of the lowest at 0.0641935,

TABLE 16 | Performance metrics of HPDE algorithm for FC7.

Sl. No.	I_{exp} (A)	V_{exp} (V)	V_{est} (V)	P_{exp} (W)	P_{est} (W)	AE_v (A)	RE (%)	MBE
1	0.2417	22.6916	22.56458	5.48456	5.45386	0.127016	0.559751	0.001076
2	1.3177	20.1869	20.35846	26.60028	26.82634	0.171557	0.849843	0.001962
3	2.6819	19.2897	19.32465	51.73305	51.82678	0.034949	0.181182	8.14E−05
4	4.0118	18.5607	18.66665	74.46182	74.88686	0.105948	0.570817	0.000748
5	5.3755	18.1682	18.13217	97.66316	97.46946	0.036034	0.198334	8.66E−05
6	6.7563	17.7196	17.66514	119.7189	119.351	0.054462	0.307356	0.000198
7	8.0689	17.271	17.2604	139.358	139.2724	0.0106	0.061375	7.49E−06
8	10.8134	16.4299	16.47266	177.6631	178.1255	0.042761	0.260265	0.000122
9	13.4556	15.7009	15.72574	211.265	211.5993	0.02484	0.158206	4.11E−05
10	16.1488	14.9907	14.9076	242.0818	240.7399	0.083097	0.554323	0.00046
11	17.5295	14.6542	14.43438	256.8808	253.0274	0.219824	1.500075	0.003222
12	18.8423	14.0374	13.92018	264.4969	262.2882	0.117222	0.835071	0.000916
13	20.2234	13.1963	13.25589	266.8741	268.0793	0.059595	0.4516	0.000237
14	21.6049	12.0187	12.30086	259.6628	265.7589	0.282164	2.347705	0.005308
15	22.9189	10.1308	10.05735	232.1868	230.5035	0.073447	0.724985	0.00036
						0.096234	0.637392	0.000988

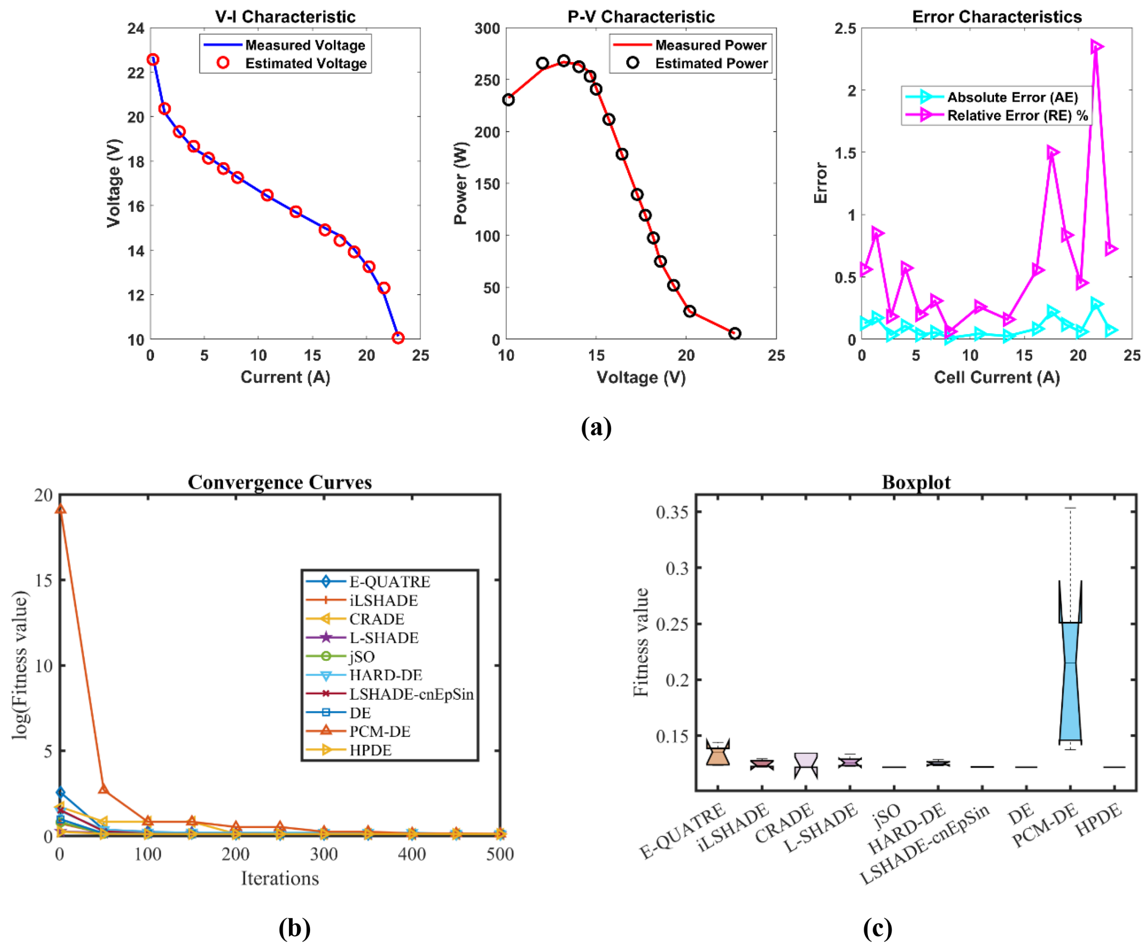

FIGURE 7 | HPDE algorithm characteristic curves of FC7: (a) $V-I$, $P-V$, and error curve; (b) convergence curve; and (c) box plot.

TABLE 17 | Parameters estimated for FC8.

Algorithm	E-QUATRE	iLSHADE	CRADE	L-SHADE	jSO	HARD-DE	LSHADE-cnEpSin	DE	PCM-DE	HPDE
ξ_1	−1.1849063	−0.8646342	−1.0062657	−0.9439126	−0.866263	−0.8718016	−0.8772558	−1.1526606	−1.1159433	−1.0448959
ξ_2	0.003685	0.0025125	0.0029701	0.0029033	0.0022669	0.0023947	0.0028537	0.0030328	0.0031152	0.0030595
ξ_3	8.807E−05	6.967E−05	7.322E−05	8.21E−05	5.037E−05	5.904E−05	9.329E−05	4.502E−05	6.128E−05	7.142E−05
ξ_4	−0.0001467	−0.0001443	−0.0001463	−0.0001466	−0.0001467	−0.0001465	−0.000146	−0.0001464	−0.000133	−0.0001464
λ	15.908533	15.011912	14.378351	14.449418	14.488436	14.448473	14.188006	14.378028	15.061415	14.397706
R_c	0.0006376	0.000522	0.0001	0.0001081	0.0001004	0.0001421	0.0001	0.0001003	0.0004384	0.0001
B	0.0241701	0.0235864	0.0239432	0.024022	0.0241531	0.0236757	0.0234952	0.0239379	0.0245648	0.0239744
Min.	0.0809762	0.0802894	0.0784938	0.0785378	0.0785193	0.0788388	0.0786674	0.0784976	0.1376584	0.0784922
Max.	0.1079498	0.0854882	0.0806994	0.0800355	0.0797348	0.0823513	0.0788486	0.0785093	0.2378285	0.0784922
Mean	0.087973	0.083093	0.0795747	0.0791644	0.0789119	0.0799228	0.0787678	0.0785018	0.1780223	0.0784922
Std.	0.0114463	0.0019637	0.0010458	0.0007026	0.0004867	0.0013861	7.652E−05	4.75E−06	0.0422313	3.67E−16
RT	2.869701	2.6844437	2.2592241	2.4282538	5.1180527	2.7635358	2.7219029	3.2315483	5.48773	0.0499442
FR	8.6	8.4	5.6	4.8	4.2	6	4.2	2.2	10	1

TABLE 18 | Performance metrics of HPDE algorithm for FC8.

Sl. No.	I_{exp} (A)	V_{exp} (V)	V_{est} (V)	P_{exp} (W)	P_{est} (W)	AE_v (A)	RE (%)	MBE
1	0.2582	23.271	23.21664	6.008572	5.994535	0.054365	0.233616	0.000197
2	1.334	21.028	21.10731	28.05135	28.15715	0.079308	0.377154	0.000419
3	2.6471	20.0748	20.11794	53.14	53.2542	0.04314	0.214895	0.000124
4	4.0281	19.4019	19.43403	78.15279	78.28224	0.032135	0.165627	6.88E−05
5	5.3919	18.8972	18.90022	101.8918	101.9081	0.003017	0.015966	6.07E−07
6	6.7726	18.5047	18.4333	125.3249	124.8413	0.071404	0.385871	0.00034
7	8.0852	18.0561	18.02927	145.9872	145.7702	0.026832	0.148603	4.8E−05
8	10.8297	17.2897	17.24932	187.2423	186.805	0.040375	0.233523	0.000109
9	13.523	16.5047	16.51247	223.1931	223.2982	0.007774	0.047104	4.03E−06
10	16.1652	15.7196	15.76837	254.1105	254.8989	0.048774	0.310275	0.000159
11	17.5459	15.3271	15.35272	268.9278	269.3773	0.025619	0.167148	4.38E−05
12	18.8584	14.9907	14.92473	282.7006	281.4565	0.06597	0.440072	0.00029
13	20.2733	14.5421	14.39848	294.8164	291.9046	0.143623	0.987636	0.001375
14	21.5523	13.5888	13.79568	292.8699	297.3287	0.206881	1.522439	0.002853
15	22.9337	12.5234	12.47932	287.2079	286.1969	0.044084	0.352017	0.00013
						0.059553	0.373463	0.000411

indicating highly consistent performance. The mean value for HPDE is 0.0641935, which is competitive and better than several other algorithms, such as PCM-DE (0.0752258) and E-QUATRE (0.0672483). The standard deviation of HPDE is impressively low at 2.19E−16, indicating exceptional stability, whereas other algorithms like PCM-DE show higher variability with a standard deviation of 0.009367. In terms of runtime, HPDE has one of the fastest RTs at 0.051231 s, significantly quicker than other algorithms like jSO (5.1489093) and PCM-DE (5.4395497). The Friedman Rank further underscores HPDE's superior performance with a rank of 1, indicating the best overall performance among the evaluated algorithms. In comparison, other algorithms like PCM-DE and E-QUATRE have higher Friedman Ranks of 9.6 and 9, respectively. In Tables 25 and 26, HDPE not only consistently outperforms other algorithms in terms of key metrics but also demonstrates unparalleled stability and efficiency, making it the most effective algorithm in this evaluation shown in Figure 12.

Comprehensive performance evaluation of the HPDE algorithm:

1. Standard Deviation: In optimization studies, standard deviation is a metric of highest importance, as it conveys the variability of the algorithm's performance across multiple runs. In the case of the HPDE algorithm, the standard deviation of results for each parameter estimation task in PEMFC models is calculated to show the consistency and stability of the algorithm. If HPDE has a low standard deviation, this means that HPDE is producing similar high quality solutions irrespective of initialization

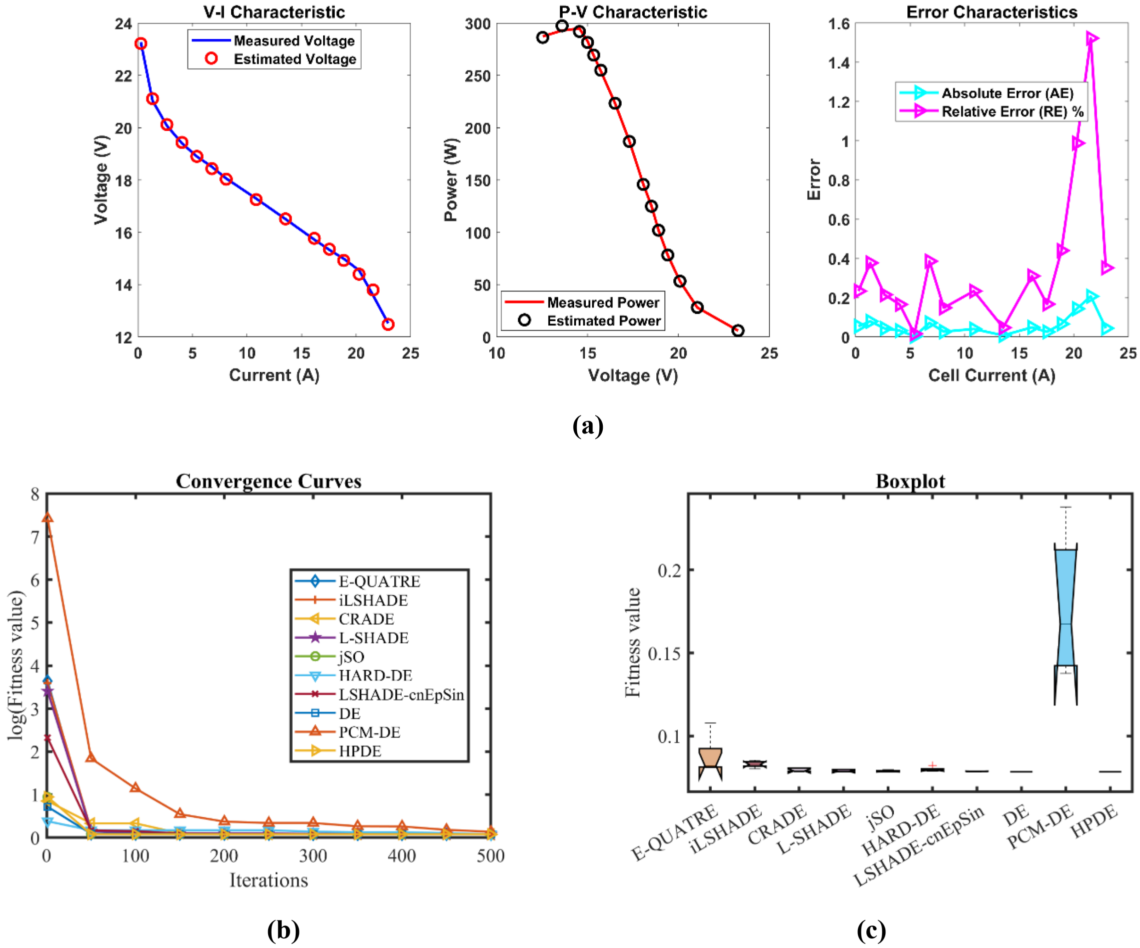

FIGURE 8 | HPDE algorithm characteristic curves of FC8: (a) $V-I$, $P-V$, and error curve; (b) convergence curve; and (c) box plot.

TABLE 19 | Parameters estimated for FC9.

Algorithm	E-QUATRE	iLSHADE	CRADE	L-SHADE	jSO	HARD-DE	LSHADE-cnEpSin	DE	PCM-DE	HPDE
ξ_1	−1.19969	−0.8557827	−0.8773549	−0.9158935	−1.0793938	−0.9626095	−1.0315854	−1.0594216	−0.9597951	−0.8730523
ξ_2	0.0034965	0.0019502	0.0027142	0.0021041	0.00271	0.002176	0.0027632	0.0031428	0.002647	0.0019209
ξ_3	8.592E−05	4.369E−05	0.000098	4.201E−05	5.207E−05	3.692E−05	6.689E−05	9.008E−05	7.322E−05	3.755E−05
ξ_4	−0.0001184	−0.0001201	−0.0001208	−0.0001209	−0.0001208	−0.0001205	−0.000121	−0.0001208	−0.0001131	−0.0001208
λ	23	22.997499	23	23	22.999827	23	23	22.999829	18.835052	23
R_c	0.0001161	0.0001806	0.0001	0.0001126	0.0001	0.0002205	0.0001001	0.0001003	0.0005117	0.0001
B	0.0632622	0.0621834	0.0624799	0.0624508	0.0624632	0.0619812	0.0626037	0.0624717	0.0591136	0.0624799
Min.	0.2033459	0.2028595	0.2023192	0.2024253	0.2023197	0.2032854	0.2024066	0.2023213	0.222275	0.2023192
Max.	0.222436	0.2068764	0.2096986	0.2049046	0.2023686	0.2083109	0.2026782	0.2023327	0.2594436	0.2023192
Mean	0.2111907	0.2040741	0.205271	0.2031103	0.2023364	0.2047157	0.2025641	0.2023244	0.2422121	0.2023192
Std.	0.0069429	0.0015964	0.0040419	0.0010561	1.89E−05	0.0021741	0.0001287	4.703E−06	0.0163137	3.627E−16
RT	2.8046815	2.6941564	2.2069663	2.3933711	5.0824901	2.8001405	2.7001406	3.2101501	5.4549681	0.0496575
FR	8.4	6.8	4.5	6	3.4	7	5	2.8	10	1.1

or random factors. During PEMFC optimization, consistent performance is critical, so HPDE's stability across different trials would demonstrate its suitability for applications where repeatability of the results is required. Finally, the standard deviation of the results of HPDE can be compared to those of other benchmark algorithms like LSHADE-cnEpSin and PCM-DE, to reinforce the claim that not only HPDE is accurate, but it is also very little variable, and therefore, a reliable tool for parameter identification in PEMFCs.

TABLE 20 | Performance metrics of HPDE algorithm for FC9.

Sl. No.	I_{exp} (A)	V_{exp} (V)	V_{est} (V)	P_{exp} (W)	P_{est} (W)	AE_v (A)	RE (%)	MBE
1	0.2046	21.5139	21.51969	4.401744	4.402928	0.005786	0.026895	2.23E−06
2	1.2619	19.6737	19.57791	24.82624	24.70536	0.095794	0.486916	0.000612
3	2.6433	18.7154	18.6624	49.47042	49.33032	0.052999	0.283184	0.000187
4	3.9734	17.9449	18.07571	71.30227	71.82204	0.130813	0.728971	0.001141
5	5.3206	17.5497	17.59286	93.37493	93.60456	0.043158	0.245917	0.000124
6	6.7019	17.1545	17.15542	114.9677	114.9739	0.000921	0.005367	5.65E−08
7	8.0491	16.6843	16.75861	134.2936	134.8917	0.074311	0.445392	0.000368
8	10.7265	15.8752	16.0031	170.2853	171.6573	0.127903	0.805675	0.001091
9	13.472	15.1411	15.212	203.9809	204.9361	0.070901	0.46827	0.000335
10	16.1494	14.4634	14.35228	233.5752	231.7807	0.111122	0.768297	0.000823
11	17.4795	14.087	13.85842	246.2337	242.2382	0.228581	1.622641	0.003483
12	18.8438	13.5792	13.26817	255.8837	250.0228	0.311027	2.290467	0.006449
13	20.1739	12.6772	12.54771	255.7486	253.1363	0.129486	1.021409	0.001118
14	21.5382	10.8743	11.47597	234.2128	247.1717	0.60167	5.53295	0.024134
15	22.9025	8.9213	8.794867	204.3201	201.4244	0.126433	1.417202	0.001066
						0.140727	1.076637	0.002729

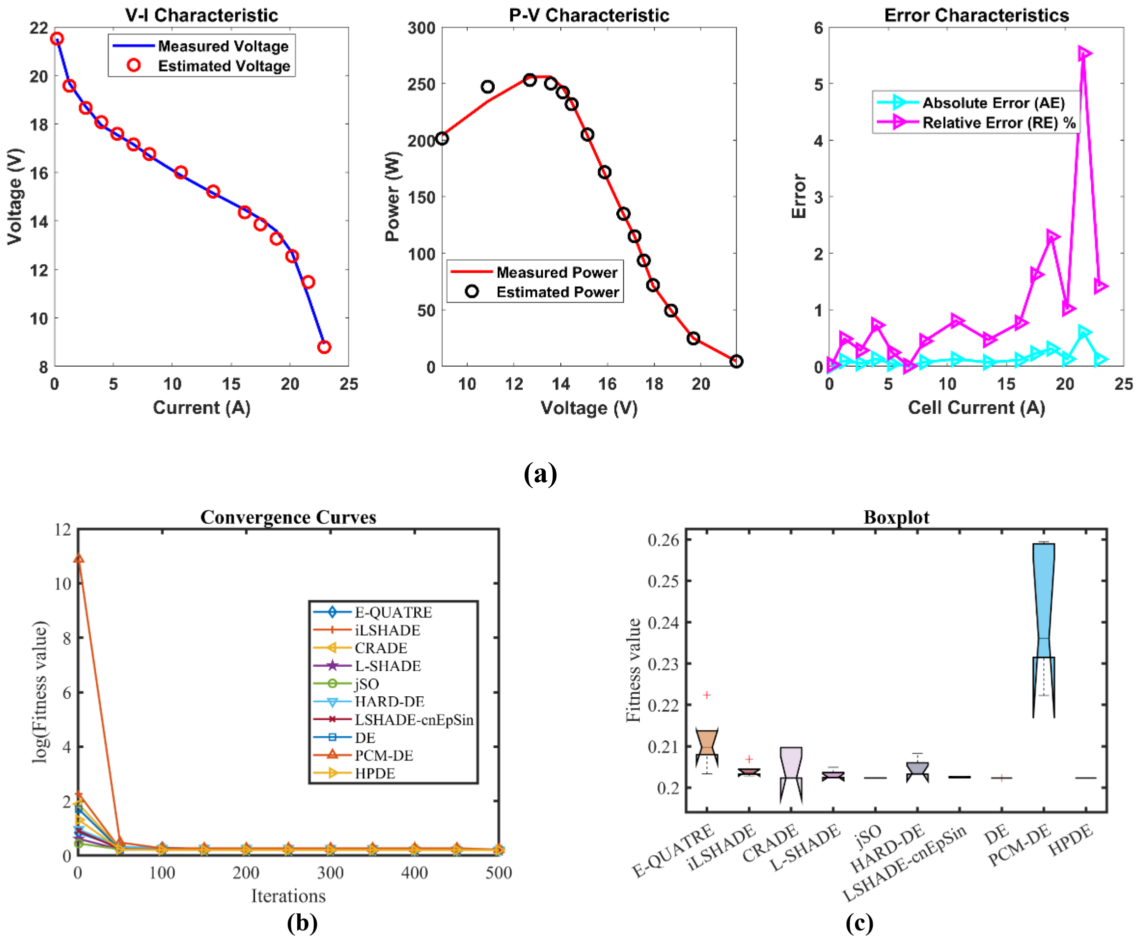

FIGURE 9 | HPDE algorithm characteristic curves of FC9: (a) $V-I$, $P-V$, and error curve; (b) convergence curve; and (c) box plot.

TABLE 21 | Parameters estimated for FC10.

Algorithm	E-QUATRE	iLSHADE	CRADE	L-SHADE	jSO	HARD-DE	LSHADE-cnEpSin	DE	PCM-DE	HPDE
ξ_1	−1.0713548	−0.8795596	−1.0921641	−0.9005385	−0.9824752	−1.1292614	−0.9764828	−0.9125945	−1.188115	−0.9710751
ξ_2	0.0028441	0.0022099	0.003302	0.0028306	0.0027954	0.0031766	0.0024351	0.0023148	0.0035676	0.0031821
ξ_3	4.833E−05	4.129E−05	7.905E−05	8.452E−05	6.392E−05	6.11E−05	3.746E−05	4.211E−05	7.89E−05	9.627E−05
ξ_4	−0.0001372	−0.0001388	−0.0001372	−0.0001381	−0.0001372	−0.0001386	−0.0001371	−0.0001372	−0.0001379	−0.0001372
λ	14	14	14	14.001875	14.000038	14	14	14.000817	14	14
R_c	0.0008	0.0006247	0.0008	0.0007429	0.0007995	0.0007953	0.0007983	0.0007998	0.0005154	0.0008
B	0.015285	0.0161226	0.0155029	0.0158219	0.0155347	0.0151986	0.0155461	0.0154981	0.0161736	0.0155029
Min.	0.1046418	0.1057369	0.1044462	0.1049773	0.1044535	0.1050301	0.1044689	0.104451	0.1105915	0.1044462
Max.	0.1126453	0.1095164	0.1446772	0.1138174	0.1050614	0.121409	0.1050507	0.1044813	0.1950521	0.1044462
Mean	0.1086723	0.1073954	0.1175799	0.1101864	0.1045829	0.1115244	0.1047601	0.1044667	0.1516124	0.1044462
Std.	0.0034365	0.0015988	0.0156071	0.0040176	0.0002676	0.0062428	0.0002413	1.277E−05	0.0318177	1.947E−16
RT	2.7850812	2.6687409	2.2554635	2.3464271	5.0056106	2.6672033	2.668026	3.1164497	5.3801302	0.0499261
FR	6	6	7.4	7.6	3	7.4	4.2	2.6	9.8	1

TABLE 22 | Performance metrics of HPDE algorithm for FC10.

Sl. No.	I_{exp} (A)	V_{exp} (V)	V_{est} (V)	P_{exp} (W)	P_{est} (W)	AE_v (A)	RE (%)	MBE
1	0.2729	23.541	23.47401	6.424339	6.406058	0.066986	0.28455	0.000299
2	1.279	21.4756	21.55584	27.46729	27.56992	0.080244	0.37365	0.000429
3	2.6603	20.3484	20.53214	54.13285	54.62165	0.18374	0.902969	0.002251
4	3.9734	19.8969	19.89719	79.05834	79.05948	0.000285	0.001434	5.43E−09
5	5.3547	19.4642	19.36756	104.225	103.7075	0.096635	0.496477	0.000623
6	6.719	19.0127	18.91713	127.7463	127.1042	0.095566	0.502645	0.000609
7	8.0321	18.5049	18.52373	148.6332	148.7844	0.018828	0.101744	2.36E−05
8	10.7265	17.8835	17.78336	191.8274	190.7532	0.100145	0.559983	0.000669
9	13.472	17.2808	17.06737	232.8069	229.9316	0.213434	1.235092	0.003037
10	16.1664	16.2089	16.35879	262.0396	264.4627	0.149886	0.924717	0.001498
11	17.4966	15.8701	15.99327	277.6728	279.8279	0.123172	0.776126	0.001011
12	18.8608	15.5312	15.59616	292.9309	294.156	0.064955	0.418225	0.000281
13	20.191	15.1923	15.17004	306.7477	306.2983	0.022259	0.146517	3.3E−05
14	21.5553	14.6282	14.64548	315.3152	315.6877	0.017279	0.118124	1.99E−05
15	22.9195	13.745	13.70153	315.0285	314.0323	0.043466	0.316228	0.000126
						0.085125	0.477232	0.000727

2. Convergence Rate: Another critical performance metric that has direct impact on applications that require fast and accurate results such as real-time PEMFC parameter optimizations, is the convergence rate of an algorithm. Faster convergence rate of an algorithm means that it faster the algorithm finds the optimal solution, and in the case where computational efficiency matters. HPDE's hierarchical population mechanism and new mutation strategies are devised to strike a good balance between exploration and exploitation, thus speeding up convergence. The study can show HPDE's efficiency in reaching near-optimal solutions by including a detailed analysis of convergence curves for HPDE and its benchmark counterparts, iLSHADE and jSO. It is evident that HPDE can greatly reduce the computational burden in PEMFC optimization when HPDE converges in fewer iterations than other algorithms, and thus, HPDE is a preferable choice for real-time applications and applications with limited processing capability.

3. Robustness: Robustness is the algorithm's ability to perform well (with the same accuracy) regardless of initial conditions or parameter configuration(s). PEMFC parameter estimation is a robust problem because the operational conditions such as temperature, humidity, and pressure are usually unpredictable and variable. Based on its unique diversity metric and adaptive population structure, HPDE is robust against premature convergence and is able to find more thoroughly the entire solution space. By evaluating HPDE's performance under different initialization schemes and control parameter settings, the study could

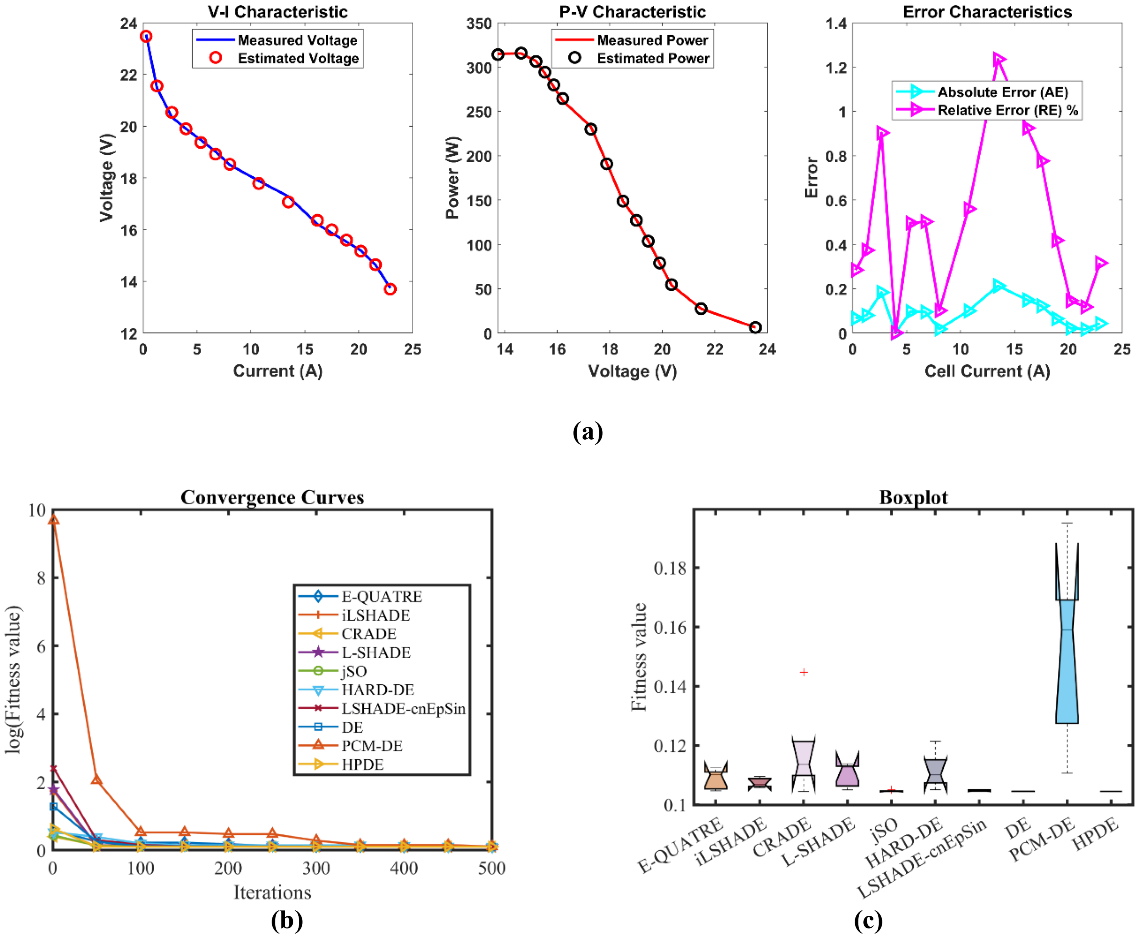

FIGURE 10 | HPDE algorithm characteristic curves of FC10: (a) $V-I$, $P-V$, and error curve; (b) convergence curve; (c) and box plot.

TABLE 23 | Parameters estimated for FC11.

Algorithm	E-QUATRE	iLSHADE	CRADE	L-SHADE	jSO	HARD-DE	LSHADE-cnEpSin	DE	PCM-DE	HPDE
ξ_1	−0.9023517	−0.8701382	−0.8532	−1.0094142	−1.1776736	−1.0328628	−1.0382422	−0.9739356	−1.19969	−0.8550426
ξ_2	0.002353	0.0018894	0.0024243	0.0021933	0.0031869	0.0025201	0.0026183	0.0025007	0.0030347	0.0015828
ξ_3	8.097E−05	5.524E−05	0.000098	4.386E−05	7.544E−05	6.189E−05	6.771E−05	7.46E−05	5.958E−05	3.667E−05
ξ_4	−0.0000954	−0.0000954	−0.0000954	−0.0000954	−9.54E−05	−0.0000954	−0.0000954	−9.54E−05	−9.639E−05	−0.0000954
λ	23	23	23	22.988435	23	23	23	22.991875	16.830307	23
R_c	0.0001	0.0001	0.0001	0.000229	0.0001	0.000222	0.0001	0.0001011	0.000485	0.0001
B	0.0354038	0.0348125	0.0348125	0.034654	0.034811	0.0347484	0.0348049	0.034806	0.0323121	0.0348125
Min.	0.0755641	0.0754843	0.0754843	0.0755348	0.0754843	0.0755367	0.0754844	0.0754862	0.0788169	0.0754843
Max.	0.0838975	0.0756701	0.0763917	0.0759818	0.0756143	0.0760775	0.0754888	0.0755138	0.1178721	0.0761032
Mean	0.0779909	0.0755524	0.0757739	0.0757074	0.0755524	0.0757221	0.0754864	0.0754947	0.0994453	0.0756081
Std.	0.0034707	9.272E−05	0.0003709	0.0001947	5.686E−05	0.0002173	1.975E−06	1.127E−05	0.0172328	0.0002768
RT	2.8027837	2.6528445	2.1649961	2.3435661	4.9699461	2.6562388	2.6633898	3.0550784	5.2673452	0.048964
FR	7.8	4.6	5.1	6.2	5	6.8	3	3.6	10	2.9

show that HPDE is able to adapt to different problem instances. Moreover, testing HPDE under fluctuating conditions of the environment, for example, temperature or pressure variations, will confirm that the algorithm can generate consistent accurate values of parameter estimates. An advantageous feature of this level of robustness would be that HPDE could be an adaptable solution in the dynamic environments that are common to PEMFC operations.

4. Error Metrics and Success Rate: Additional error metrics, such as mean absolute error (MAE), mean relative error

TABLE 24 | Performance metrics of HPDE algorithm for FC11.

Sl. No.	I_{exp} (A)	V_{exp} (V)	V_{est} (V)	P_{exp} (W)	P_{est} (W)	AE_v (A)	RE (%)	MBE
1	0.104	9.53	9.707993	0.99112	1.009631	0.177993	1.867713	0.002112
2	0.199	9.38	9.438403	1.86662	1.878242	0.058403	0.622629	0.000227
3	0.307	9.2	9.24429	2.8244	2.837997	0.04429	0.481416	0.000131
4	0.403	9.24	9.11262	3.72372	3.672386	0.12738	1.378576	0.001082
5	0.511	9.1	8.988224	4.6501	4.592983	0.111776	1.228303	0.000833
6	0.614	8.94	8.88339	5.48916	5.454402	0.05661	0.633221	0.000214
7	0.704	8.84	8.7986	6.22336	6.194214	0.0414	0.468324	0.000114
8	0.806	8.75	8.707212	7.0525	7.018013	0.042788	0.489	0.000122
9	0.908	8.66	8.618541	7.86328	7.825635	0.041459	0.478741	0.000115
10	1.075	8.45	8.474219	9.08375	9.109785	0.024219	0.286611	3.91E−05
11	1.126	8.41	8.429358	9.46966	9.491457	0.019358	0.23018	2.5E−05
12	1.28	8.2	8.288062	10.496	10.60872	0.088062	1.073928	0.000517
13	1.39	8.14	8.178151	11.3146	11.36763	0.038151	0.468687	9.7E−05
14	1.45	8.11	8.113272	11.7595	11.76424	0.003272	0.040343	7.14E−07
15	1.57	8	7.96769	12.56	12.50927	0.03231	0.403869	6.96E−05
						0.060498	0.676769	0.00038

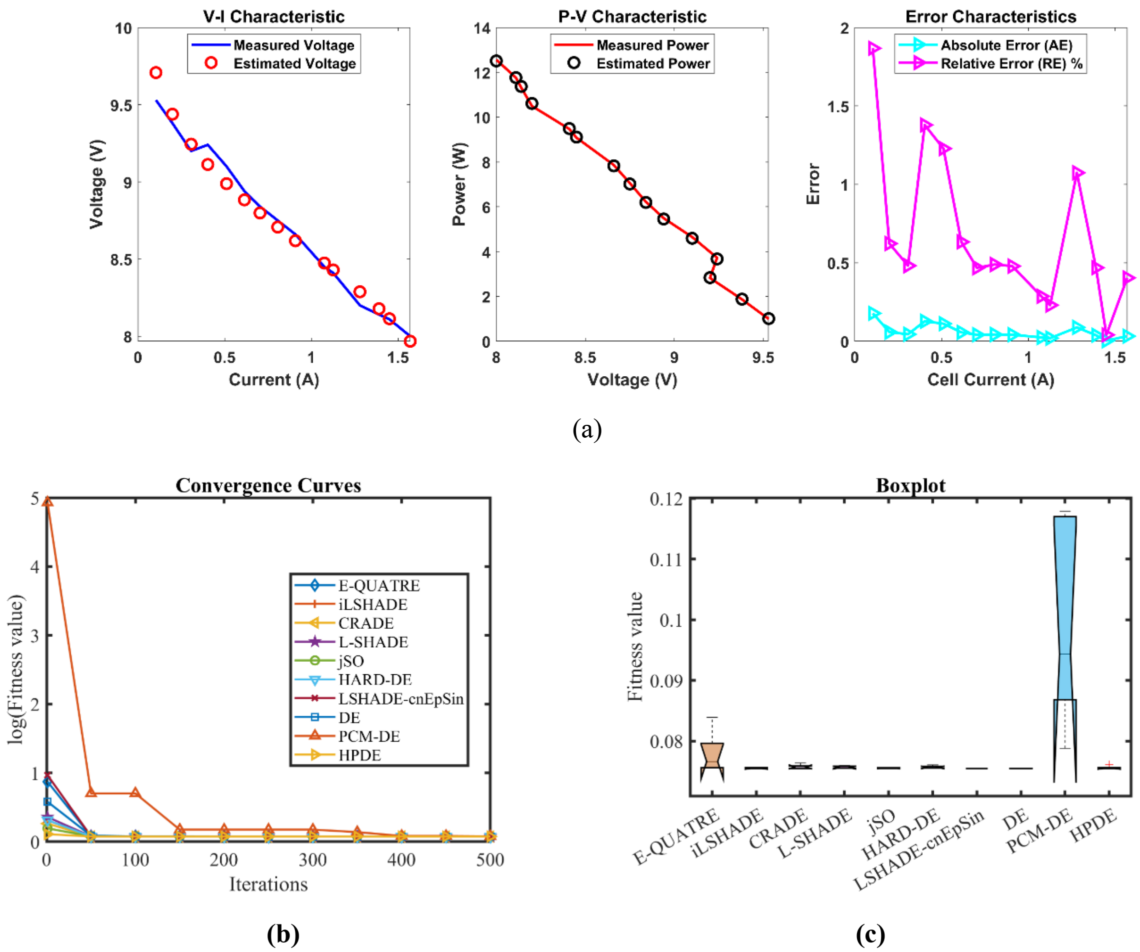

FIGURE 11 | HPDE algorithm characteristic curves of FC11: (a) $V-I$, $P-V$, and error curve; (b) convergence curve; and (c) box plot.

TABLE 25 | Parameters estimated for FC12.

Algorithm	E-QUATRE	iLSHADE	CRADE	L-SHADE	jSO	HARD-DE	LSHADE-cnEpSin	DE	PCM-DE	HPDE
ξ_1	−1.0694156	−0.853214	−0.9375441	−1.1870939	−0.8760021	−1.19969	−1.1972638	−0.9782898	−1.0422284	−0.9479441
ξ_2	0.0030782	0.0020085	0.002745	0.003281	0.0021411	0.0027862	0.0034367	0.0020876	0.0025471	0.0020459
ξ_3	9.159E−05	6.44E−05	0.000098	7.9E−05	6.87E−05	4.045E−05	8.785E−05	4.121E−05	5.998E−05	4.521E−05
ξ_4	−0.0000954	−0.0000954	−0.0000954	−0.0000954	−9.54E−05	−0.0000954	−0.0000954	−9.54E−05	−9.839E−05	−0.0000954
λ	23	14	14	14.81819	15.135808	14.908717	14	14.009606	16.602701	14
R_c	0.0001455	0.0007926	0.0008	0.0003635	0.0005083	0.0001162	0.0008	0.0004413	0.000558	0.0008
B	0.0513428	0.0484914	0.0484826	0.049162	0.0492197	0.0494618	0.0485626	0.0488881	0.0498953	0.0484826
Min.	0.0642567	0.0641936	0.0641935	0.0642098	0.0642081	0.0642173	0.0641944	0.0641979	0.0681297	0.0641935
Max.	0.0722812	0.0642004	0.1070005	0.0642327	0.0642552	0.0643694	0.0642009	0.0642265	0.0882686	0.0641935
Mean	0.0672483	0.0641972	0.0727848	0.0642214	0.0642255	0.0642656	0.0641972	0.0642052	0.0752258	0.0641935
Std.	0.0040914	2.691E−06	0.0191272	9.669E−06	1.833E−05	6.185E−05	2.457E−06	1.204E−05	0.009367	2.191E−16
RT	2.7515627	2.6017652	2.2365729	2.4025535	5.1489093	2.6846616	2.6548737	3.1879523	5.4395497	0.051231
FR	9	3	6.8	5.6	6	7	2.8	4.2	9.6	1

TABLE 26 | Performance metrics of HPDE algorithm for FC12.

Sl. No.	I_{exp} (A)	V_{exp} (V)	V_{est} (V)	P_{exp} (W)	P_{est} (W)	AE_v (A)	RE (%)	MBE
1	0.097	9.87	9.999678	0.95739	0.969969	0.129678	1.313858	0.001121
2	0.115	9.84	9.926759	1.1316	1.141577	0.086759	0.881696	0.000502
3	0.165	9.77	9.767165	1.61205	1.611582	0.002835	0.029016	5.36E−07
4	0.204	9.7	9.669213	1.9788	1.972519	0.030787	0.317393	6.32E−05
5	0.249	9.61	9.573415	2.39289	2.38378	0.036585	0.380701	8.92E−05
6	0.273	9.59	9.527681	2.61807	2.601057	0.062319	0.649835	0.000259
7	0.326	9.5	9.436219	3.097	3.076208	0.063781	0.671375	0.000271
8	0.396	9.4	9.32984	3.7224	3.694616	0.07016	0.746388	0.000328
9	0.5	9.26	9.191101	4.63	4.595551	0.068899	0.744048	0.000316
10	0.621	9.05	9.04691	5.62005	5.618131	0.00309	0.034147	6.37E−07
11	0.711	8.93	8.946524	6.34923	6.360979	0.016524	0.185043	1.82E−05
12	0.797	8.83	8.853563	7.03751	7.05629	0.023563	0.266855	3.7E−05
13	1.006	8.54	8.630282	8.59124	8.682064	0.090282	1.057172	0.000543
14	1.141	8.42	8.481149	9.60722	9.676991	0.061149	0.72623	0.000249
15	1.37	8.27	8.200536	11.3299	11.23473	0.069464	0.839953	0.000322
						0.054392	0.589581	0.000275

(MRE), and mean bias error (MBE), are also used to further support HPDE's precision and reliability for PEMFC optimization. Each error metric gives a different view of the algorithm's performance. For example, MAE and MRE tell you how far, on average, the estimated parameter deviates from the corresponding actual parameter, whereas MBE can reveal the existence of systematic bias in the estimation procedure. The study would present these metrics to provide a complete view of HPDE's accuracy relative to CRADE and HARD-DE algorithms. In addition, judging the success rate (the fraction of trials where HPDE does find solutions within a certain error threshold) would confirm HPDE's ability to arrive at high-quality solutions in most trials. If HPDE has a high success rate in HPDE, then it is a reliable means to achieve PEMFC parameter optimization goals and is therefore a strong candidate for applications where precision and consistency are required.

5. Comparative Statistical Analysis: comparative tests, such as the Friedman rank test, are then performed to statistically confirm the performance advantages of HPDE over the other algorithms. These tests would enable a quantitative comparison of all metrics, with statistical evidence that HPDE clearly outperforms its competitors. Performance distribution and convergence characteristics of HPDE w.r.t. other algorithms could be visualized using box plots and convergence curves. HPDE's accelerated convergence towards optimal solutions can be visualized on the convergence curves, whereas the stability of the trials is exposed by box plots on standard deviation and error metrics. These

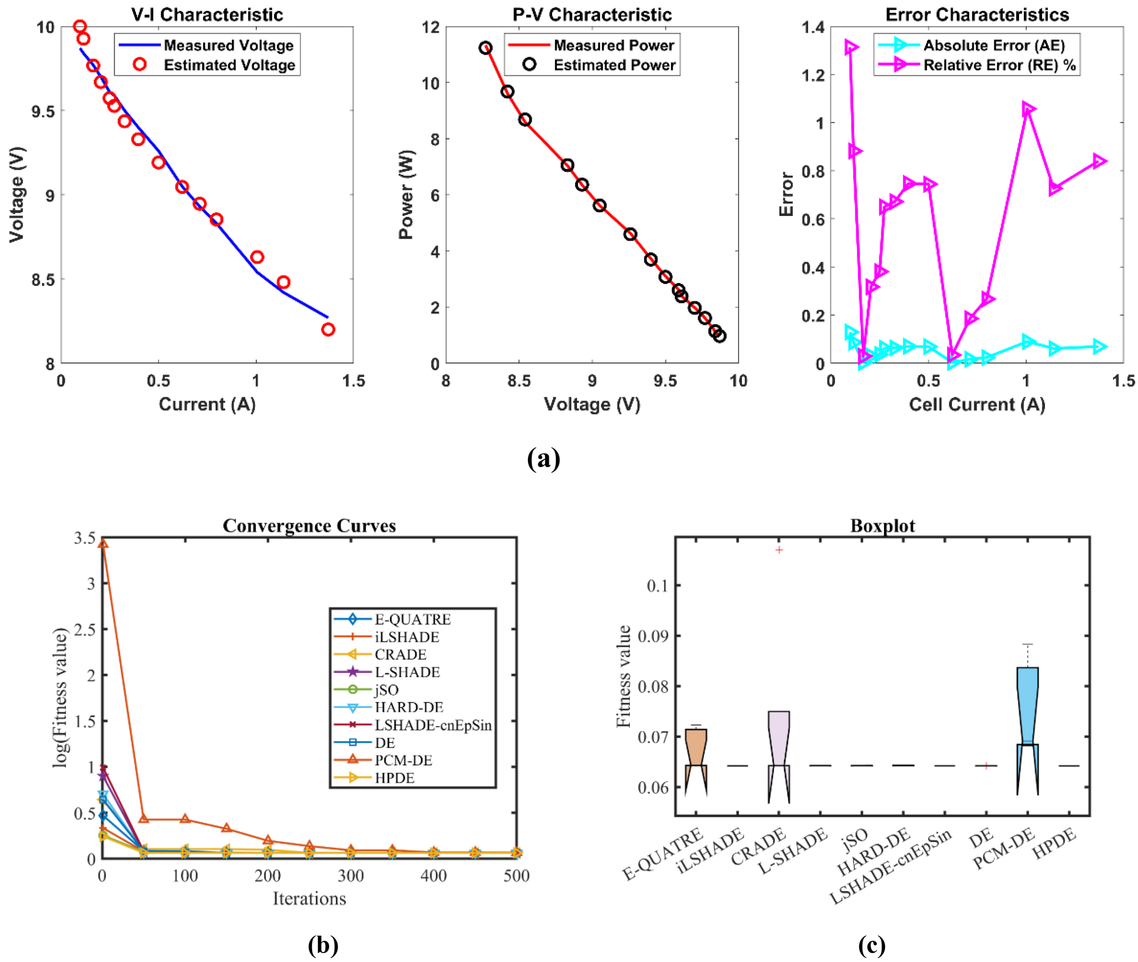

FIGURE 12 | HPDE algorithm characteristic curves of FC11: (a) $V-I$, $P-V$, and error curve; (b) convergence curve; and (c) and box plot.

statistical comparisons, and the visual representations of these clearly answer the reviewers' request for a deeper analysis of HPDE performance and strength.

5 | Conclusion

This study concludes that the HPDE algorithm is a very effective tool for optimizing parameters in PEMFCs. It is shown that HPDE consistently outperforms established DE variants and other advanced EAs in terms of precision, stability, and efficiency for different performance metrics. The algorithm was benchmarked against leading DE variants (E-QUATRE, iLSHADE, CRADE, L-SHADE, jSO, HARD-DE, LSHADE-cnEpSin, DE, and PCM-DE), and other EAs (PSO and GA variations). HPDE is shown to achieve up to a 40% improvement in solution quality (as measured by a lower Sum of Squared Errors, SSE) and up to a 60% faster convergence rate, on average, compared to these algorithms.

The dynamic hierarchical population structure and ranking-based mutation strategies are key to HPDE's success in the effective exploration and exploitation of the complex, multivariable optimization landscape of PEMFC models. The SSE values of HPDE are consistently lower than those of competing algorithms, and HPDE reduces the standard deviation by over 70% compared to competing algorithms, demonstrating HPDE's stability on various PEMFC models and operating conditions. More specifically, HPDE yields the lowest values in terms of Absolute Error (AE), Relative Error (RE), and Mean Bias Error (MBE), and thus can serve as a valid tool in capturing PEMFC characteristics with accuracy.

The superior performance of HPDE has important implications for the design, control and operational efficiency of PEMFCs, and makes HPDE an advanced tool for engineers and researchers in sustainable energy. HPDE is used to develop optimized fuel cell systems, which are necessary to improve fuel cell reliability and performance, by providing precise parameter estimates. In addition to providing HPDE as a benchmark for PEMFC optimization, this study demonstrates the wider potential of HPDE to motivate further innovation in metaheuristic optimization techniques for complex energy systems.

Nomenclature

$C(\mu_F, 0.1)$	a semi-fixed Cauchy distribution with mean μ_F and scale 0.1, used to generate scaling factor F for population exploration in the ordinary layer

CR_i	the crossover rate for the ith individual, drawn from a Gaussian distribution with mean μ_{CR} and variance 0.1, controlling the extent of crossover
IS	individual status, quantifying individual performance within the population, calculated by comparing an individual's fitness with the generation's best and worst
$V_{\lim}$	hypervolume bound representing the search space limits
V_{pop}	population diversity metric based on the spatial range in each dimension, calculated as $V_{pop} = \sqrt{\prod_{d=1}^{D} y_d}$, where y_d is the range between maximum and minimum values in dimension d
d_{VOL}	diversity metric indicating population diversity relative to initial diversity, defined as $d_{VOL} = \sqrt{\frac{V_{pop}}{V_{\lim}}}$
p_w	selection probability determining the likelihood of choosing an individual from elite or ordinary layers, calculated as $p_w = \frac{ps_{ini} - ps}{ps_{ini}}$
$X_{(r_o,G)}$ and $X_{(r_e,G)}$	randomly selected individuals from the ordinary (r_o) and elite (r_e) layers, respectively, guiding mutation and crossover strategies to maintain exploration-exploitation balance
F_{div}	diversity improvement factor from a Cauchy distribution, used to expand search diversity when needed, particularly in mutation strategies
R_h	success rate metric for each parameter pair (μ_F, μ_{CR}), calculated as $R_h = \frac{n_{s,h}^2}{n_s \cdot (n_{s,h} + n_{f,h})}$, where $n_{s,h}$ and $n_{f,h}$ denote successful and failed individual counts using the pair
Δloc_i	measures dimensional improvements between the trial vector $U_{(i,G)}$ and the target vector $X_{(i,G)}$, aiding in parameter tuning to control convergence
ps	adaptive population size, dynamically reduced based on function evaluations, with size determined by specific reduction formulas for early or later stages of evolution

Author Contributions

Mohammad Khishe: conceptualization, investigation, validation, writing – original draft, resources. **Pradeep Jangir:** funding acquisition, writing – original draft, validation, formal analysis. validation, visualization, project administration. **Sunilkumar P. Agrawal:** writing – review and editing, software, data curation. **Sundaram B. Pandya:** conceptualization, visualization, formal analysis, supervision. **Anil Parmar:** resources, formal analysis, validation, writing – original draft, methodology. **Laith Abualigah:** writing – review and editing, visualization, validation, resources, methodology.

Ethics Statement

The authors have nothing to report.

Consent

The authors have nothing to report.

Conflicts of Interest

The authors declare no conflicts of interest.

Data Availability Statement

The data presented in this study are available through email upon request to the corresponding author.

References

1. P. Barnoon, D. Toghraie, B. Mehmandoust, M. A. Fazilati, and S. A. Eftekhari, "Comprehensive Study on Hydrogen Production via Propane Steam Reforminginside a Reactor," *Energy Reports* 7 (2021): 929–941, https://doi.org/10.1016/j.egyr.2021.02.001.

2. P. Sharma, S. R. Salkuti, and S.-C. Kim, "Advancements in Energy Storage Technologies for Smart Grid Development," *International Journal of Electrical and Computer Engineering* 12, no. 4 (2022): 3421, https://doi.org/10.11591/ijece.v12i4.pp3421-3429.

3. S. Hamdollahi and L. Jun, "A Review on Modeling of Proton Exchange Membrane Fuel Cell," *Chemical Industry and Chemical Engineering Quarterly* 29, no. 1 (2023): 61–74, https://doi.org/10.2298/CICEQ220126014H.

4. U. Mitra, A. Arya, and S. Gupta, "A Comprehensive and Comparative Review on Parameter Estimation Methods for Modelling Proton Exchange Membrane Fuel Cell," *Fuel* 335 (2023): 127080, https://doi.org/10.1016/j.fuel.2022.127080.

5. T. Wilberforce, H. Rezk, A. Olabi, E. I. Epelle, and M. A. Abdelkareem, "Comparative Analysis on Parametric Estimation of a PEM Fuel Cell Using Metaheuristics Algorithms," *Energy* 262 (2023): 125530, https://doi.org/10.1016/j.energy.2022.125530.

6. S. A. Korkmaz, S. A. Çetinkaya, O. Yuksel, O. Konur, K. E. Erginer, and C. O. Colpan, "Comparison of Various Metaheuristic Algorithms to Extract the Optimal PEMFC Modeling Parameters," *International Journal of Hydrogen Energy* 51 (2024): 1402–1420.

7. B. Yang, J. Wang, L. Yu, et al., "A Critical Survey on Proton Exchange Membrane Fuel Cell Parameter Estimation Using Meta-Heuristic Algorithms," *Journal of Cleaner Production* 265 (2020): 121660, https://doi.org/10.1016/j.jclepro.2020.121660.

8. X. D. Xue, K. W. E. Cheng, and D. Sutanto, "Unified Mathematical Modelling of Steady-State and Dynamic Voltage-Current Characteristics for PEM Fuel Cells," *Electrochimica Acta* 52 (2006): 1135–1144, https://doi.org/10.1016/j.electacta.2006.07.011.

9. K. Ettihir, L. Boulon, M. Becherif, K. Agbossou, and H. Ramadan, "Online Identification of Semi-Empirical Model Parameters for PEMFCs," *International Journal of Hydrogen Energy* 39 (2014): 21165–21176, https://doi.org/10.1016/j.ijhydene.2014.10.045.

10. M. Ye, X. Wang, and Y. Xu, "Parameter Identification for Proton Exchange Membrane Fuel Cell Model Using Particle Swarm Optimization," *International Journal of Hydrogen Energy* 34 (2009): 981–989, https://doi.org/10.1016/j.ijhydene.2008.11.026.

11. R. Salim, M. Nabag, H. Noura, and A. A. Fardoun, "The Parameter Identification of the Nexa 1.2 kW PEMFC's Model Using Particle Swarm Optimization," *Renewable Energy* 82 (2015): 26–34, https://doi.org/10.1016/j.renene.2014.10.012.

12. P. Bhatt, N. Agarwal, and U. K. Chakraborty, "Parameter Optimization of PEMFC With Genetic Algorithm," *New Mathematics and Natural Computation* 12, no. 3 (2016): 241–249, https://doi.org/10.1142/S1793005716500162.

13. P. Kumar, S. K. Kannaiah, S. R. Choudhury, and N. Rajasekar, "Genetic Algorithm-Based Modeling of PEM Fuel Cells Suitable for Integration in DC Microgrids," *Electric Power Components & Systems* 45, no. 10 (2017): 1152–1160, https://doi.org/10.1080/15325008.2017.1318980.

14. K. Priya, T. S. Babu, K. Balasubramanian, K. S. Kumar, and N. Rajasekar, "A Novel Approach for Fuel Cell Parameter Estimation Using Simple Genetic Algorithm," *Sustainable Energy Technologies and Assessments* 12 (2015): 46–52, https://doi.org/10.1016/j.seta.2015.09.001.

15. K. Balasubramanian, B. Jacob, K. Priya, K. Sangeetha, N. Rajasekar, and T. S. Babu, "Critical Evaluation of Genetic Algorithm Based Fuel Cell Parameter Extraction," *Energy Procedia* 75 (2015): 1975–1982, https://doi.org/10.1016/j.egypro.2015.07.244.

16. W. Gong, X. Yan, X. Liu, and Z. Cai, "Parameter Extraction of Different Fuel Cell Models With Transferred Adaptive Differential Evolution," *Energy* 86 (2015): 139–151, https://doi.org/10.1016/j.energy.2015.03.117.

17. S. S. Khan, M. A. Rafiq, H. Shareef, and M. K. Sultan, "Parameter Optimization of PEMFC Model Using Backtracking Search Algorithm," in *5th International Conference on Renewable Energy: Generation and Applications (ICREGA)* (IEEE, 2018), 323–326, https://doi.org/10.1109/ICREGA.2018.8337625.

18. M. Ali, M. El-Hameed, and M. Farahat, "Effective Parameters' Identification for Polyme Electrolyte Membrane Fuel Cell Models Using Grey Wolf Optimizer," *Renewable Energy* 111 (2017): 455–462, https://doi.org/10.1016/j.renene.2017.04.036.

19. P. Hao and B. Sobhani, "Application of the Improved Chaotic Grey Wolf Optimization Algorithm as a Novel and Efficient Method for Parameter Estimation of Solid Oxide Fuel Cells Model," *International Journal of Hydrogen Energy* 46, no. 73 (2021): 36454–36465, https://doi.org/10.1016/j.ijhydene.2021.08.174.

20. A. Abdullah, H. Rezk, A. Hadad, M. Hassan, and A. Mohamed, "Optimal Parameter Estimation of Proton Exchange Membrane Fuel Cells," *Intelligent Automation & Soft Computing* 29 (2021): 619–631, https://doi.org/10.32604/iasc.2021.018289.

21. A. A. El-Fergany, "Extracting Optimal Parameters of PEM Fuel Cells Using Salp Swarm Optimizer," *Renewable Energy* 119 (2018): 641–648, https://doi.org/10.1016/j.renene.2017.12.051.

22. B. Yang, D. Li, C. Zeng, Y. Han, and J. Li, "Bald Eagle Search Algorithm for Parameter Identification of Proton Exchange Membrane Fuel Cell," *Frontiers in Energy Research* 10 (2022): 885461, https://doi.org/10.3389/fenrg.2022.885461.

23. H. Rezk, A. G. Olabi, S. Ferahtia, and E. T. Sayed, "Accurate Parameter Estimation Methodology Applied to Model Proton Exchange Membrane Fuel Cell," *Energy* 255 (2022): 124454, https://doi.org/10.1016/j.energy.2022.124454.

24. Z. Yang, Q. Liu, L. Z. Zhang, J. Dai, and N. Razmjooy, "Model Parameter Estimation of the PEMFCs Using Improved Barnacles Mating Optimization Algorithm," *Energy* 212 (2020): 1–10, https://doi.org/10.1016/j.energy.2020.118738.

25. J. Gupta, P. Nijhawan, and S. Ganguli, "Optimal Parameter Estimation of PEM Fuel Cell Using Slime Mould Algorithm," *International Journal of Energy Research* 45 (2021): 14732–14744, https://doi.org/10.1002/er.6750.

26. A. Diab, M. Tolba, A. El-Magd, M. Zaky, and A. El-Rifaie, "Fuel Cell Parameters Estimation via Marine Predators and Political Optimizers," *IEEE Access* 8 (2020): 166998–167018, https://doi.org/10.1109/ACCESS.2020.3021754.

27. M. A. Shaheen, H. M. Hasanien, M. S. El Moursi, and A. A. El-Fergany, "Precise Modeling of PEM Fuel Cell Using Improved Chaotic MayFly Optimization Algorithm," *International Journal of Energy Research* 45 (2021): 18754–18769, https://doi.org/10.1002/er.6987.

28. H. Sultan, A. Menesy, S. Kamel, and F. Jurado, "Tree Growth Algorithm for Parameter Identification of Proton Exchange Membrane Fuel Cell Models," *International Journal of Interactive Multimedia and Artificial Intelligence* 6 (2020): 101–111, https://doi.org/10.9781/jimai.2020.03.003.

29. M. Danoune, A. Djafour, Y. Wang, and A. Gougui, "The Whale Optimization Algorithm for Efficient PEM Fuel Cells Modeling," *International Journal of Hydrogen Energy* 46 (2021): 37599–37611, https://doi.org/10.1016/j.ijhydene.2021.03.105.

30. G. Zhang, C. Xiao, and N. Razmjooy, "Optimal Parameter Extraction of PEM Fuel Cells by Meta-Heuristics," *International Journal of Ambient Energy* 43.1 (2022): 2510–2519.

31. A. Askarzadeh and A. Rezazadeh, "A New Artificial Bee Swarm Algorithm for Optimization of Proton Exchange Membrane Fuel Cell Model Parameters," *Journal of Zhejiang University. Science. A* 12 (2011): 638–646, https://doi.org/10.1631/jzus.C1000355.

32. A. S. Menesy, H. M. Sultan, A. Korashy, S. Kamel, and F. Jurado, "A Modified Farmland Fertility Optimizer for Parameters Estimation of Fuel Cell Models," *Neural Computing and Applications* 33 (2021): 12169–12190, https://doi.org/10.1007/s00521-021-05821-1.

33. Z. Yuan, W. Wang, H. Wang, and N. Razmjooy, "A New Technique for Optimal Estimation of the Circuit-Based PEMFCs Using Developed Sunflower Optimization Algorithm," *Energy Reports* 6 (2020): 662–671, https://doi.org/10.1016/j.egyr.2020.03.010.

34. Y. Song, X. Tan, and S. Mizzi, "Optimal Parameter Extraction of the Proton Exchange Membrane Fuel Cells Based on a New Harris Hawks Optimization Algorithm," *Energy Sources, Part A: Recovery, Utilization, and Environmental Effects* 46 (2020): 1–18, https://doi.org/10.1080/15567036.2020.1769230.

35. S. R. Fahim, H. M. Hasanien, R. A. Turky, et al., "Parameter Identification of Proton Exchange Membrane Fuel Cell Based on Hunger Games Search Algorithm," *Energies* 14, no. 5022 (2021): 1–21, https://doi.org/10.3390/en14165022.

36. E. A. Gouda, M. F. Kotb, and A. A. El-Fergany, "Investigating Dynamic Performances of Fue Cells Using Pathfinder Algorithm," *Energy Conversion and Management* 237 (2021): 114099, https://doi.org/10.1016/j.enconman.2021.114099.

37. M. Singla, P. Nijhawan, and A. S. Oberoi, "Parameter Estimation of Proton Exchange Membrane Fuel Cell Using a Novel Meta-Heuristic Algorithm," *Environmental Science and Pollution Research* 28 (2021): 1–16, https://doi.org/10.1007/s11356-021-13097-0.

38. Z. Mat Isa, N. Mohd Nayan, M. Arshad, and N. A. Mohamad Kajaan, "Optimizing PEMFC Model Parameters Using Ant Lion Optimizer and Dragonfly Algorithm: A Comparative Study," *International Journal of Electrical and Computer Engineering* 9 (2019): 5295, https://doi.org/10.11591/ijece.v9i6.pp5295-5303.

39. T. Wang, H. Huang, X. Li, X. Guo, M. Liu, and H. Lei, "Optimal Estimation of Proton Exchange Membrane Fuel Cell Model Parameters Based on an Improved Chicken Swarm Optimization Algorithm," *International Journal of Green Energy* 20 (2022): 946–965, https://doi.org/10.1080/15435075.2022.2131432.

40. L. Liu and G. Fathi, "A Metaheuristic-Based Methodology for Efficient System Identification of the Proton Exchange Membrane Fuel Cell Stacks," *International Journal of Hydrogen Energy* 47 (2022): 39626–39638, https://doi.org/10.1016/j.ijhydene.2022.09.129.

41. S. Li, X. Fang, J. Liao, M. Ghadamyari, M. Khayatnezhad, and N. Ghadimi, "Evaluating the Efficiency of CCHP Systems in Xinjiang Uygur Autonomous Region: An Optimal Strategy Based on Improved Mother Optimization Algorithm," *Case Studies in Thermal Engineering* 54 (2024): 104005.

42. W. Jiang, X. Wang, H. Huang, D. Zhang, and N. Ghadimi, "Optimal Economic Scheduling of Microgrids Considering Renewable Energy Sources Based on Energy Hub Model Using Demand Response and Improved Water Wave Optimization Algorithm," *Journal of Energy Storage* 55 (2022): 105311.

43. L. Chen, H. Huang, P. Tang, D. Yao, H. Yang, and N. Ghadimi, "Optimal Modeling of Combined Cooling, Heating, and Power Systems Using Developed African Vulture Optimization: A Case Study in Watersport Complex," *Energy Sources, Part A: Recovery, Utilization, and Environmental Effects* 44, no. 2 (2022): 4296–4317.

44. E. Han and N. Ghadimi, "Model Identification of Proton-Exchange Membrane Fuel Cells Based on a Hybrid Convolutional Neural Network and Extreme Learning Machine Optimized by Improved Honey Badger Algorithm," *Sustainable Energy Technologies and Assessments* 52 (2022): 102005.

45. G. Bo, P. Cheng, K. Dezhi, et al., "Optimum Structure of a Combined Wind/Photovoltaic/Fuel Cell-Based on Amended Dragon Fly Optimization Algorithm: A Case Study," *Energy Sources, Part A: Recovery, Utilization, and Environmental Effects* 44, no. 3 (2022): 7109–7131.

46. M. Ghiasi, Z. Wang, M. Mehrandezh, S. Jalilian, and N. Ghadimi, "Evolution of Smart Grids Towards the Internet of Energy: Concept and Essential Components for Deep Decarbonisation," *IET Smart Grid* 6, no. 1 (2023): 86–102.

47. Q. Li, S. Tianle, L. Yin, et al., "Health Management for PEMFC System Long-Term Operation Based on Optimal Temperature Trajectory Real-Time Optimization," *IEEE Transactions on Industrial Electronics* (2024): 1–11.

48. Q. Li, H. Wang, T. Wang, et al., "Online Diagnosis Method of Water Management Faults Based on Hybrid-Frequency Electrochemical Impedance Spectroscopy for PEMFC," *IEEE Transactions on Transportation Electrification* (2024).

49. Z. Meng and Q. Zhang, "HPDE: A Dynamic Hierarchical Population Based Differential Evolution With Novel Diversity Metric," *Engineering Applications of Artificial Intelligence* 126 (2023): 106989, https://doi.org/10.1016/j.engappai.2023.106989.

50. Z. Meng, Y. Chen, X. Li, C. Yang, and Y. Zhong, "Enhancing QUasi-Affine TRansformation Evolution (QUATRE) With Adaptation Scheme on Numerical Optimization," *Knowledge-Based Systems* 197 (2020): 105908, https://doi.org/10.1016/j.knosys.2020.105908.

51. J. Brest, M. S. Maučec, and B. Bošković, "iL-SHADE: Improved L-SHADE Algorithm for Single Objective Real-Parameter Optimization," in *2016 IEEE Congress on Evolutionary Computation (CEC)* (Vancouver, British Columbia, Canada: IEEE, 2016), 1188–1195, https://doi.org/10.1109/CEC.2016.7743922.

52. Y. Li, J. Liang, C. Yue, K. Yu, X. Ban, and P. Chen, "Collaborative Resource Allocation-Based Differential Evolution for Solving Numerical Optimization Problems," *Information Sciences* 660 (2024): 120104, https://doi.org/10.1016/j.ins.2024.120104.

53. R. Tanabe and A. S. Fukunaga, "Improving the Search Performance of Shade Using Linear Population Size Reduction," in *2014 IEEE Congress on Evolutionary Computation (CEC)* (Beijing, China: IEEE, 2014), 1658–1665, https://doi.org/10.1109/CEC.2014.6900380.

54. Z. Meng and J.-S. Pan, "HARD-DE: Hierarchical Archive Based Mutation Strategy With Depth Information of Evolution for the Enhancement of Differential Evolution on Numerical Optimization," *IEEE Access* 7 (2019): 12832–12854, https://doi.org/10.1109/ACCESS.2019.2893292.

55. N. H. Awad, M. Z. Ali, and P. N. Suganthan, "Ensemble Sinusoidal Differential Covariance Matrix Adaptation With Euclidean Neighborhood for Solving CEC2017 Benchmark Problems," in *2017 IEEE Congress on Evolutionary Computation (CEC)* (Donostia, San Sebastián, Spain: IEEE, 2017), 372–379, https://doi.org/10.1109/CEC.2017.7969336.

56. D. G. Mayer, B. P. Kinghorn, and A. A. Archer, "Differential Evolution—An Easy and Efficient Evolutionary Algorithm for Model Optimisation," *Agricultural Systems* 83, no. 3 (2005): 315–328, https://doi.org/10.1016/j.agsy.2004.05.002.

57. Z. Song, C. Ren, and Z. Meng, "Differential Evolution With Perturbation Mechanism and Covariance Matrix Based Stagnation Indicator for Numerical Optimization," *Swarm and Evolutionary Computation* 84 (2024): 101447, https://doi.org/10.1016/j.swevo.2023.101447.

58. H. M. Sultan, A. S. Menesy, M. Hassan, F. Jurado, and S. Kamel, "Standard and Quasi Oppositional Bonobo Optimizers for Parameter Extraction of PEM Fuel Cell Stacks," *Fuel* 340 (2023): 127586, https://doi.org/10.1016/j.fuel.2023.127586.

59. H. Zhou, X. Wu, Y. Li, et al., "Model Optimization of a High-Power Commercial PEMFC System via an Improved Grey Wolf Optimization Method," *Fuel* 357 (2024): 129589, https://doi.org/10.1016/j.fuel.2023.129589.

60. A. S. Menesy, H. M. Sultan, A. Selim, M. G. Ashmawy, and S. Kamel, "Developing and Applying Chaotic Harris Hawks Optimization Technique for Extracting Parameters of Several Proton Exchange Membrane Fuel Cell Stacks," *IEEE Access* 8 (2020): 1146–1159, https://doi.org/10.1109/ACCESS.2019.2961811.

61. C. Yongguang and Z. Guanglei, "New Parameters Identification of Proton Exchange Membrane Fuel Cell Stacks Based on an Improved Version of African Vulture Optimization Algorithm," *Energy Reports* 8, no. 75 (2022): 3030–3040, https://doi.org/10.1016/j.egyr.2022.02.066.

62. Z.-J. Mo, X.-J. Zhu, L.-Y. Wei, and G.-Y. Cao, "Parameter Optimization for a PEMFC Model With a Hybrid Genetic Algorithm," *International Journal of Energy Research* 30 (2006): 585–597, https://doi.org/10.1002/er.1170.

63. J. Corrêa, F. Farret, V. Popov, and M. Simoes, "Sensitivity Analysis of the Modeling Parameters Used in Simulation of Proton Exchange Membrane Fuel Cells," *IEEE Transactions on Energy Conversion* 20, no. 1 (2005): 211–218, https://doi.org/10.1109/TEC.2004.842382.

64. J. Corrêa, F. Farret, L. Canha, and M. Simoes, "An Electrochemical-Based Fuel-Cell Model Suitable for Electrical Engineering Automation Approach," *IEEE Transactions on Industrial Electronics* 51, no. 5 (2004): 1103–1112, https://doi.org/10.1109/TIE.2004.834972.

65. J. C. Amphlett, R. M. Baumert, R. F. Mann, B. A. Peppley, P. R. Roberge, and T. J. Harris, "Performance Modeling of the Ballard Mark IV Solid Polymer Electrolyte Fuel Cell," *Journal of the Electrochemical Society* 142, no. 1 (1995): 1–15, https://doi.org/10.1149/1.2043959.

66. U. K. Chakraborty, T. E. Abbott, and S. K. Das, "PEM Fuel Cell Modeling Using Differential Evolution," *Energy* 40, no. 1 (2012): 387–399, https://doi.org/10.1016/j.energy.2012.01.039.

67. R. F. Mann, J. C. Amphlett, M. A. Hooper, H. M. Jensen, B. A. Peppley, and P. R. Roberge, "Development and Application of a Generalised Steady-State Electrochemical Model for a PEM Fuel Cell," *Journal of Power Sources* 86, no. 1 (2000): 173–180, https://doi.org/10.1016/S0378-7753(99)00484-X.

68. J. Thepkaew, A. Therdthianwong, and S. Therdthianwong, "Key Parameters of Active Layers Affecting Proton Exchange Membrane (PEM) Fuel Cell Performance," *Energy* 33, no. 12 (2008): 1794–1800, https://doi.org/10.1016/j.energy.2008.08.008.

69. M. Ohenoja and K. Leiviskä, "Validation of Genetic Algorithm Results in a Fuel Cell Model," *International Journal of Hydrogen Energy* 35, no. 22 (2010): 12618–12625, https://doi.org/10.1016/j.ijhydene.2010.07.129.

70. S. Yang and N. Wang, "A Novel P Systems Based Optimization Algorithm for Parameter Estimation of Proton Exchange Membrane Fuel Cell Model," *International Journal of Hydrogen Energy* 37, no. 10 (2012): 8465–8476, https://doi.org/10.1016/j.ijhydene.2012.02.131.